NOTICE

The quality of this microform is heavily dependent upon the quality of the original thesis submitted for microfilming. Every effort has been made to ensure the highest quality of reproduction possible.

If pages are missing, contact the university which granted the degree.

Some pages may have indistinct print especially if the original pages were typed with a poor typewriter ribbon or if the university sent us an inferior photocopy.

Reproduction in full or in part of this microform is governed by the Canadian Copyright Act, R.S.C. 1970, c. C-30, and subsequent amendments.

AVIS

La qualité de cette microforme dépend grandement de la qualité de la thèse soumise au microfilmage. Nous avons tout fait pour assurer une qualité supérieure de reproduction.

S'il manque des pages, veuillez communiquer avec l'université qui a conféré le grade.

La qualité d'impression de certaines pages peut laisser à désirer, surtout si les pages originales ont été dactylographiées à l'aide d'un ruban usé ou si l'université nous a fait parvenir une photocopie de qualité inférieure.

La reproduction, même partielle, de cette microforme est soumise à la Loi canadienne sur le droit d'auteur, SRC 1970, c. C-30, et ses amendements subséquents.

ISBN 0-315-56101-7

Canada

A Fluorescence Polarization Probe of the Dissociation of γγ Enolase

Daniel J. Trepanier

A Thesis

in

The Department

of

Chemistry

Presented in Partial Fulfilment of the Requirements
for the Degree of Master of Science at
Concordia University
Montreal, Quebec, Canada

November 1989

ABSTRACT

A Fluorescence Polarization Probe of the
Dissociation of γγ Enolase

Daniel J. Trepanier

The dimeric isozyme of rabbit brain enolase, γγ, (2-phospho-D-glycerate hydrolase E.C. 4.2.1.11) was covalently labelled with fluorescein isothiocyanate (FITC) and the fluorescence polarization of the labelled enzyme species (γγ-FITC) was used as a probe of dissociation.

γγ-FITC was shown to remain dimeric and to fully retain the specific activity characteristic of the unlabelled enzyme.

In the presence of 0.5 Molar sodium perchlorate ($NaClO_4$) both γγ and γγ-FITC are fully dissociated and a concomitant 15% decrease in the fluorescence polarization, relative to that of the dimer, is observed.

The decrease in polarization is shown to be a result of the increased rotational motion of the monomer, relative to the dimer, as well as an increased flexibility of FITC at its site of binding. It is anticipated that this same 15% decrease in polarization would be observed under other conditions that promoted the dissociation of γγ-FITC.

TABLE OF CONTENTS

Section D:

INTRODUCTION:

Enolase (2-phospho-D-glycerate hydratase, EC 4.2.1.11) is a glycolytic enzyme which catalyses the dehydration of 2 phosphoglyceric acid (2-PGA) to form phosphoenolpyruvate (PEP).

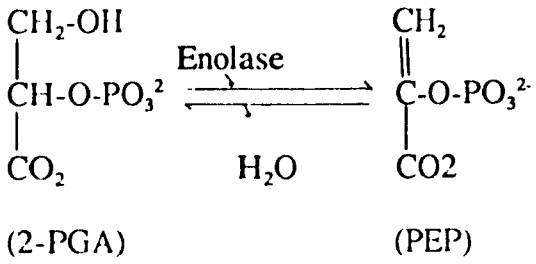

Mammals posses 3 distinct subunits of enolase α, β and γ, which arise from 3 distinct genes. These subunits, of 40000 to 50000 daltons [1,2,3], associate to form dimers. 5 of the 6 possible combinations have been found in vivo [4,5]. The work described here is concerned only with the 91000 dalton γγ dimer [6] from rabbit brain.

The regulation of the activity of oligomeric enzymes is known to not be restricted solely at the level of the tertiary structure but also includes subunit interactions imposed by the quaternary structure [7]. In this regard it is necessary to establish the extent to which the quaternary structure contributes to the observed activity of the oligomer. Ideally, then, one would want to be able to observe the activity of the oligomeric and monomeric structures independent of any damaging perturbations that might result due to the process of generating

these species.

Biochemically this has been achieved in cases where the oligomer owes its existence to weak subunit interactions and as such a simple decrease in protein concentration results in dissociation, thereby enabling one to observe the native activity of the subunits.

In most cases, however, dissociation does not occur upon dilution and one must therefore use a chemical (salt, denaturants, pH, detergents etc.) or physical (temperature or pressure) perturbant to generate the dissociated subunits of the oligomer. Since each oligomer has it's own number and type of subunit contacts and tertiary structural forces, the effect of the chemical or physical perturbants will depend upon the specific protein under study. This has resulted, as illustrated by the 2 examples discussed below, in unambiguous data when active subunits are found and generally inconclusive evidence when inactive or partially active subunits result.

In the simplest case, that of a dimer(D)-monomer(M) equilibrium, 3 models can be introduced:

(1) $D \rightleftharpoons 2M$

(2) $D \rightleftharpoons 2M^{*}$

(3) $D \rightleftharpoons 2M \rightleftharpoons 2M^{\mp}$

In the first model dissociation does not lead to a change in the tertiary structure of the monomer (M), whereas in the second model the structure of the

monomer has been altered (M^*) as a result of the dissociation. In the third model, dissociation is followed by an effect of the chemical or physical agent on the structure of the monomer ($M^{\ddagger}$).

Borschik and coworkers [7] have concluded that the quaternary structure of E.Coli inorganic pyrophosphatase is not required for catalytic activity. The enzyme is a hexamer of identical 20Kdal subunits and catalyzes the hydrolysis of inorganic pyrophosphate in the presence of divalent metals. In 20% isopropanol the enzyme is completely dissociated into monomeric subunits as evidenced by a decrease in the sedimentation coefficient and the presence of a single protein fraction, during gel filtration, with an elution volume corresponding to 20Kdal. Upon dilution into an assay mixture containing the substrate the sedimentation coefficient characteristic of the monomer is maintained and the enzyme retains full activity and identical kinetic parameters (Km and Vmax). In this case then, the results led to only one conclusion.

Porter and Cardenas [8] have used enzyme immobilization to demonstrate that the monomers of the tetramer pyruvate kinase are inactive or at most partially active. In this technique the oligomer is covalently coupled to a cyanogen bromide activated sepharose matrix via a single subunit. The oligomer is treated with a denaturing agent and the dissociated subunits are washed away leaving only the covalently bound and denatured monomer. The monomer is allowed to renature upon removal of the denaturant and any recovered activity is measured.

A common criticism of this method is that the immobilized subunit may be prevented from folding correctly because of interactions with the matrix, and as such results in a false assessment of activity.

In 1969, Gawronski and Westhead [9], concluded that yeast enolase is both dissociated and inactivated in 1M solutions of KCl and KBr. It was concluded that the dimeric structure is essential for catalytic activity. This statement, however, assumes that the high salt has acted solely through a shift in the equilibrium towards the monomeric species, and consequently that the tertiary structure of the monomer has been uneffected, aside from any intrinsic structural alteration due to dissociation itself (model 1 or 2). If this assumption is true then the yeast monomers are indeed inactive.

In 1971, Nagy and Orman [10], reported that the yeast enolase monomers were active when one uses low enzyme concentration and a temperature of 43°C. On a sephadex G-75 column in the absence and presence of 1 M KBr, yeast enolase eluted as the 66000 dalton dimer and the inactive 33000 dalton monomer, respectively, as monitored by the tryptophan absorbance at 280 nm. The concentration of yeast enolase was lowered (in the presence of substrate) and the temperature raised to 43°C. Under these conditions the elution of the enzyme was detected via it's activity and was found to elute as the 33000 dalton monomer. One could then conclude that the monomer was active and that Gawronski and Westhead had been dealing with a structurally altered inactive monomer due to the presence of 1M salt (model 3).

In 1978, Marangos [11], showed that mammalian enolases were inactive in a 1 M solution of KBr. The technique of subunit scrambling was used to demonstrate that in the presence of the salt the isozymes were monomeric. The technique makes use of the fact that αα, αγ and γγ can be separated from each other on a DEAE cellulose column. Equal concentrations of αα and γγ were incubated together in the presence of 1 M KBr. The KBr was dialysed away and the solution applied to the column. It was found that equal concentrations of all the isozymes were recovered. Consequently it was concluded that the salt resulted in dissociation and since no activity was to be found, that the monomers were inactive. Considering the results of the yeast enolase experiments, then, the finding that mammalian enolase monomers are inactive in 1M KBr does not necessarily mean that they are intrinsically inactive since the results could equally be explained by an effect of the salt on the structure of the monomer (model 3).

At this point we are confronted with experimental limitations since it is known that γγ does not undergo a concentration dependant dissociation in the concentration range where spectroscopic instrumentation can be used to establish catalytic activity.[unpublished ultrafiltration results conducted in our laboratory]. To determine if the γ monomer is active we must then use some method other than dilution of γγ or incubation of γγ with high salt to generate the monomers.

In 1981, Paladini and Weber [12], found that under pressure, yeast enolase was fully dissociated by 2000 bar. Application of pressure to an

oligomeric protein solution is expected to result in dissociation owing to the increased solvation of the dissociated species, which favourably decreases the solution volume. This increased solvation of, for instance, a monomer relative to a dimer is thought to be due to the accessability of extra solvation sites at the dimer subunit interface that become exposed upon dissociation to the monomer [12].

The sample under study was placed within a pressure bomb [12] equipped with four quartz windows (90 degrees apart). This apparatus was then placed within an absorption or fluorescence spectrophotometer and the fluorescence polarization of an extrinsic probe was used, under pressure, to relay the equilibrium state of the enzyme.

The technique of fluorescence polarization (a detailed treatment of the theory is presented in the appendix) basically involves the excitation of a fluorescence species with plane polarized light. For macromolecules, such as an enzyme, the fluorescent species can be either intrinsic (ex. tryptophan) or extrinsic (covalent attachment of a small fluorescent molecule,or probe, to the enzyme) to the enzyme. During the lifetime of the excited state of the fluorescent molecule, the macromolecule will undergo rotational motion such that the light emitted from the excited state will be at an angle to the original plane of excitation. This angle, then, is a measure of the degree of rotation. One says that the light has been depolarized. Since the rotational rate of a low molecular weight macromolecule will be faster than that of a high molecular weight

macromolecule, the monomer of yeast enolase will rotate faster than the dimer. The monomer will, consequently, be expected to increase the degree of depolarization, during the lifetime of the excited state of the fluorescent molecule, to a greater extent than the dimer. Consequently, as one dissociates the dimer, towards monomers, we will observe a decrease in the polarization. Since the lifetime of tryptophan is short and its emission is weak, an extrinsic fluorescent probe is generally used for fluorescence polarization studies on macromolecules.

In this way, then, Paladini and Weber were able to show that yeast enolase was fully dissociated by 2000 bar and that within less than 5 minutes after pressure release the polarization characteristic of the dimer was reestablished. Since the reassociation, upon pressure release is within the same timescale as that required to make an activity measurement, no such measurements were conducted.

In 1982, Kornblatt, Kornblatt and Hui Bon Hoa [13] demonstrated the pressure induced reversible inactivation of $\alpha\alpha$, $\alpha\gamma$, and $\gamma\gamma$. A loss of activity, however does not distinguish between;

(A) Activity loss due to dimer inactivation.

and/

(B) Activity loss due to dissociation of the dimer.

This left a number of possibilities for the pressure induced activity loss.

(1) Dissociation occurs at very low pressure, giving active monomers; the inactivation is due to high pressure-induced denaturation of the monomer.
(2) Pressure causes dissociation of the enzyme into monomers which are inactive or partially active.
3) Pressure causes conformational changes in the dimer, which leads to loss of activity without dissociation.

In 1987, Kornblatt and Hui Bon Hoa [14] obtained evidence of the quaternary structure of αα, αγ, and γγ under pressure, using subunit scrambling (the formation of αα and γγ from the dissociation of αγ, or vice versa), and glutaraldehyde crosslinking (covalent attachment of the monomers by the use of the bifunctional reagent, glutaraldehyde). It was concluded that the isozymes underwent pressure induced dissociation. The isozymes did not differ in the pressure required to initiate dissociation (1200 bar) but the α and γ subunits did differ in their stabilities towards pressure. The results indicated that the α monomer was unstable over the pressure range that produces dissociation of αα and that the γ monomer was stable over this pressure range (1200-2000 bar).

Since subunit scrambling cannot be performed on γγ alone, and since the α monomer is unstable (unable to reassociate) at pressures required for dissociation, it could not be determined whether the dissociation of γγ was complete.

The experiments were also time consuming and laborious, since a different enzyme sample was used for each pressure studied and was

subsequently applied to an ion exchange column to separate the various isozymes which then had their activities measured in order to determine whether dissociation had occurred under the specific pressure chosen.

My work emanates from the need for a sensitive, rapid and direct measure of the quaternary structure of enolase under pressure and under other conditions. To this end, a fluorescence polarization probe of dissociation will be developed which will be used directly under pressure, by other workers, to relay information regarding the quaternary state of $\gamma\gamma$ over a number of pressure ranges. It is anticipated that at some specific pressure range only γ monomers will exist and, since it is now possible to make a liquid (substrate) injection directly into a sample (enzyme), under pressure, within the pressure bomb, the question of intrinsic activity of the monomer can then be addressed.
The research will begin with the labelling of $\gamma\gamma$ with fluorescein isothiocyanate (FITC), to generate the $\gamma\gamma$-FITC species, and characterization of this species. We will then use salt to dissociate the $\gamma\gamma$-FITC and monitor changes in the polarization of FITC.

If we are interested in establishing a fluorescence polarization probe of dissociation, then we ideally want a situation in which any polarization changes upon dissociation are due to dissociation alone. If the change in polarization is solely due to dissociation then this same change should also be observed under pressure, if it resulted in dissociation. Experiments will, consequently, be conducted to establish whether nondissociating factors contribute to the

polarization upon salt dissociation.

It will be shown that a 15% decrease in polarization is observed upon complete dissociation of γγ-FITC, and that this change is due to dissociation and to an increase in the flexibility of FITC attachment to the monomer upon dissociation.

Polarization does not, in theory, encompass fluorescence emission. Fluorescence emission, using polarized light, is more correctly described by the parameter of "anisotropy ". Polarization and anisotropy data, however, describe the same phenomena. The polarization parameter was introduced in the original literature and most theory was presented using this term. Polarization is still widely used but the use of anisotropy is increasing. In terms of theory presentation, anisotropy is less complicated (clearer) and, consequently it will be generally stressed in the appendix and the work stated here. The experimental work itself, however, was conducted using the polarization parameter and as such the data are presented in terms of polarization.

MATERIALS AND METHODS:

BASIC:

Source of enolase.

Enolase,γγ, was purified from frozen rabbit brains (Pel-Freeze, U.S.A.) following the procedure of Kornblatt [6] and stored in 50% glycerol at - 20°C.

Activity measurement.

Two different assay buffers were used:

(1) Enolase assay buffer (pH 7.1):

50 mM Imidazole

250 mM KCL

1 mM Magnesium acetate

0.1 mM EDTA

(2) Buffer A (pH 7.15):

25 mM MES (2[Nmorpholino]ethanesulfonic acid)

25 mM TRIS (tris[hydroxymethyl]aminomethane)

100 mM Ammonium chloride

1 mM Magnesium acetate

0.1 mM EDTA (ethylenediamine tetraacetate)

The reaction in both assay media was initiated by the addition of 1 mM 2-phosphoglyceric acid (PGA). The production of phosphoenolpyruvate (PEP) was followed spectrophotometrically at 240 nm with the sample compartment thermostated at 25°C.

Identical activities of γγ are observed in the above buffers.

Protein assay.

Protein concentrations were determined with Bio-Rad Protein Assay (Bio-Rad) using bovine serum albumin as a standard.

SECTION A:

Labelling of γγ with FITC.

A solution of γγ, 1.8 mg/ml (1 ml), was dialyzed against 1 liter of HEPES buffer at 25°C for 2 hours.

HEPES buffer (ph 8.0):

25 mM HEPES (N-2-hydroxyethylpiperazine-N'-2 ethanesulfonic acid)

0.1 M KCl

5 mM magnesium acetate

0.1 mM EDTA

The contents were removed and 15 µl of 100 mM PGA was added. After ≈ 5 minutes, 1 mg of FITC was added. This solution was allowed to gently stir, in the dark, at 25°C, for ≈ 2 hours. The mixture was then placed onto a K 9/30 (9 mm x 30 cm) Pharmacia column of G-25 sephadex (super fine, Pharmacia) equilibrated in buffer A and eluted with the same buffer (with 5 mM magnesium acetate). 0.5 ml fractions were collected and assayed for activity. The active fractions were pooled and dialyzed overnight, at 5°C, against 1 liter of buffer A (with 5 mM magnesium acetate). 1 volume of glycerol was added and the γγ-FITC solution was stored at -20°C.

Absorption spectra of FITC and γγ-FITC.

For γγ-FITC:

After the labelling procedure but prior to storage in glycerol, γγ was scanned, at 25°C, from 250 nm to 600 nm, on a Cary 2290 spectrophotometer. The baseline was set using buffer A (with 5 mM magnesium acetate).

For FITC:

A solution of FITC was prepared, in buffer A, such that its absorbance at 492 nm was ≈ that of γγ-FITC. This solution was scanned, at 25°C, from 250 nm to 600 nm. The baseline was as for γγ-FITC.

Emission spectra of FITC and γγ-FITC.

For γγ-FITC (50-60 nM in buffer A):

The signal gain was set at 1.5 and the slits were 8 nM on a Perkin-Elmer MPF-44B fluorometer with a xenon lamp power supply and temperature equilibrated at 25°C. For the emission spectrum the excitation was set at 492 nm and for the excitation spectrum the emission was set at 520 nm.

For FITC:

A solution of FITC in buffer A was prepared by the addition of dry FITC to buffer A such that when the signal gain on the fluorometer was 1.5 the intensity was ≈ that of γγ-FITC. Excitation and emission spectra were obtained as for γγ-FITC.

Polarization of FITC and γγ-FITC.

For polarization of the above samples the signal gain was increased to 3.0. Fluorescence polarization was determined using **Kodak** lenses (see appendix 1.1). Polarization is calculated automatically, through the use of a differential corrected spectral unit (DCSU) connected to the fluorometer, using the equation;

$$P = \frac{I_{\parallel} - G\, I_{\perp}}{I_{\parallel} + G\, I_{\perp}}$$ (see appendix 1.0)

where; $I_{\parallel}$ is the intensity observed for both vertical excitation and emission.

$I_{\perp}$ is the intensity observed for vertical excitation and horizontal emission.

G represents a correction factor consisting of the ratio of the intensities of horizontal to vertically polarized emission with the excitation in the horizontal plane.

For both FITC and γγ-FITC the excitation and emission wavelengths were 492 nm and 520 nm, respectively. G = 0.87

Gel filtration of γγ, γγ-FITC.

A 10 mm x 32 cm column was filled with sephacryl S-200 equilibrated in buffer A at 25°C. The column was attached to a peristaltic pump and run at 5 ml/hour. Fractions (0.5 ml), eluted with buffer A, were collected using a fraction collector equipped with a drop counter.

200 µl samples of the following compounds, Blue Dextran (6 mg/ml), BSA (20 mg/ml), egg albumin (25 mg/ml), γγ (0.2 mg/ml), γγ-FITC (0.2 mg/ml), all in buffer A, were applied to the column.

Elution of Blue Dextran, BSA and egg albumin was monitored by absorbance at 280 nm. Elution of γγ was monitored by its activity and that of γγ-FITC by its activity and emission at 520 nm.

SECTION B:

Fluorescent lifetime measurement of γγ-FITC in buffer A.

The emission decay of 1 µM γγ-FITC in buffer A was measured using a picosecond laser system. The sample was excited at 355 nm (pulse width of

26.6 picoseconds/channel and signal gain of 5) and the emission was collected at 520 nm with a 495 nm cutoff filter. The digital printout of the fluorescence intensity at each channel (average of 3 decays) was used to determine the lifetime, by using the simplex method of the software package "french curve" (LEDS Publishing Company) to calculate the best fit to the single exponential decay.

Polarization of FITC and γγ-FITC versus viscosity.

Solutions of glycerol in buffer A were prepared gravimetrically. 25 µl of FITC (10 µM) or γγ-FITC (10 µM) was added to 2.5 ml of glycerol solution. The viscosities of these solutions, at 25°C, were obtained from tables [15]. The polarization was measured, at an excitation wavelength of 492 nm and emission wavelength of 520 nm with slits of 8 nm and G = 0.87, in a 25°C temperature regulated sample holder.

SECTION C:

Fluorescent lifetime measurement of γγ-FITC in $NaClO_4$.

Exactly the same procedure as for the measurement in the absence of $NaClO_4$ (section B).

Glutaraldehyde cross-linking and SDS-PAGE.

Two sample tubes were prepared containing 1.5 μM γγ (1 ml) in Enolase assay buffer minus KCl (see "basic" section of materials and methods). At time = zero minutes, 100 μl of water (tube 1) or 6 M $NaClO_4$ was added and a 75 μl aliquot removed and immediately cross-linked by glutaraldehyde (see below). Additional aliquots were removed and cross-linked at 30, 60, and 120 minutes. The tubes were then placed on ice and 100 μl of water was added to tube # 1 and 100 μl of a 3 M KCl solution (in water) was added to tube # 2 to precipitate out the perchlorate ($KClO_4$ is only slightly soluble in water). After 2 hours, 75 μl aliquots were removed from the tubes and cross-linked by glutaraldehyde.

Glutaraldehyde cross linking: To the removed aliquots (75 μl), 10 μl of glutaraldehyde (1:4 dilution with water) was added. After 1 minute of incubation, 10 μl of $NaBH_4$ (38 mg/ml), was added to terminate the reaction. 100 μl of sample buffer (2x concentrated) was added and the sample kept at room temperature until the completion of the time course.

Sample Buffer (ph 6.8):

65 mM TRIS

1.2% mercaptoethanol (v/v)

40% sucrose (w/v)

4% SDS (w/v)

0.002% bromophenol blue

All of the reaction tubes were then placed in a boiling water bath for 3 minutes. 80 µl was removed from each tube and placed into the wells of a standard SDS-PAGE (slab gel, 10% acrylamide) apparatus [16].

The running buffer was:

0.025 M TRIS

0.19 M glycine

0.1% SDS

The gel was then stained by immersion in an isopropanol-acetic acid-water solution containing 0.05% coomassie blue for 45 minutes followed by destaining in 10% acetic acid.

Gel filtration of γγ and γγ-FITC in the presence of $NaClO_4$.

Same procedure as section A of materials and methods except:

(1) The column was equilibrated and run using buffer A that also contains 0.6 M $NaClO_4$.

and/

(2) The collected fractions of γγ and γγ-FITC (0.5 ml) were diluted 10 fold with buffer A to lower the $NaClO_4$ concentration and thereby induce reassociation of the monomers. After 1 hour the fractions were assayed for

activity (γγ and γγ-FITC) and for emission at 520 nm (γγ-FITC).

Polarization of γγ-FITC versus time in NaCl and $NaClO_4$.

Buffer A containing 0.5 M $NaClO_4$, ph 7.15, was diluted with buffer A, ph 7.15 to give final concentrations of 0.4, 0.3, 0.2, and 0.1 M $NaClO_4$. To 2.5 ml of each of these solutions an aliquot of γγ-FITC was added (100 µl, in this case) (final concentration of γγ-FITC = 90 nM). The polarization was then measured as a function of time in a 25°C temperature regulated sample holder, at an excitation of 492 nm and an emission of 520 nm with slits = 8 nm and g = 0.87. The same procedure was followed for NaCl.

SECTION D:

Emission spectra of γγ-FITC versus the excitational wavelength.

A sample of γγ-FITC (90 nM) in buffer A + 0.5 M $NaClO_4$, pH 7.15, was prepared. The sample was excited with wavelengths from 450 to 500 nm and the emission was scanned in each case. The temperature was regulated at 25°C.

Excitation polarization spectra of γγ-FITC.

A sample of γγ-FITC (90 nM) in buffer A, pH 7.15 was prepared. The sample was excited with wavelengths from 450 to 500 and the polarization taken with the emission wavelength set at 520 nm. Temperature was maintained

at 25°C.

Polarization of γγ-FITC versus viscosity in $NaClO_4$.

The procedure was exactly as in section B, with the exception that buffer A + $NaClO_4$ was used to prepare the solutions of 0 to 30% glycerol by weight. As we increase the amount of glycerol in the prepared samples we also increase the dilution of our stock of 0.5 M $NaClO_4$ and as such the concentration of $NaClO_4$ in the buffer used was increased proportionally, by taking into account the density of glycerol at 25°C (1.26201 g / ml), and the volume of buffer to be added. In this way the concentration of $NaClO_4$ at each viscosity remained at approximately 0.5 M.

Activity of γγ-FITC in the presence or absence of NaCl or $NaClO_4$.

γγ-FITC was incubated for 30 minutes, at 25°C, in buffer A with varying amounts of $NaClO_4$ or NaCl. The substrate (PGA) was then added and the activity recorded.

Tryptophan emission of γγ in buffer, NaCl, urea and $NaClO_4$.

Solutions of γγ-FITC (90 nM), in buffer A, buffer A + 0.5 M NaCl and buffer A + 0.5 M $NaClO_4$ were incubated at 25°C for 30 minutes. The urea incubation was for 60 minutes. All samples were then excited at 285 nm and the emission, from 300 to 380, was scanned. The spectra observed were then

corrected for the observed raman peak, and any fluorescence, of the buffer system, in the emission range studied.

Section A: FORMATION AND CHARACTERIZATION OF γγ-FITC.

For the purposes of extrinsic fluorescence polarization, the fluorescent molecule, or probe, is usually chosen so that it can be excited by light that only the probe (not the macromolecule) can absorb. The long wavelengths of absorption and emission minimizes the problems of background fluorescence from biological samples [17].

Fluorescein isothiocyanate (FITC), excitation maximum 490nm, has been used to monitor the dissociation of malate dehydrogenase (70000 daltons) [18] and citrate synthase (100000 daltons) [19]. FITC, besides having a fluorescent lifetime 4- 5nsec) which is not negligible on the macromolecular rotational time scale, is resistant to photobleaching and is not significantly environment sensitive in terms of its absorption and emission spectra [17].

The labelling of γγ with FITC was carried out according to the procedure outlined in materials and methods.

The purpose of the experiments described in this section is twofold.

(1) To establish that γγ has been covalently labelled with FITC (γγ-FITC). and/

(2) To ascertain whether FITC attachment measurably perturbs the structure of γγ.

A:1.0: Establishment of the existence γγ-FITC.

The absorption spectrum of FITC (fig.1) exhibits an absorption maxima centered at 492 nm. The absorption spectrum of γγ (fig.1), taken after the labelling procedure displays absorption maxima at 280nm, and at 492nm. Since G-25 gel filtration followed by dialysis is assumed to remove any noncovalently bound FITC from that bound to γγ, figure 1 provides strong evidence for a γγ-FITC species.

Excitation and emission spectra of FITC and the labelled-γγ are identical (fig.2), as would be expected if the γγ contained FITC.

The inset of figure 2 shows us that the polarization of FITC is 0.023 ± 0.001 whereas that of the proposed γγ-FITC species is 0.253 ± 0.001. This much increased polarization value is expected to occur upon FITC bonding to γγ due to the decreased rotational motion of FITC once it is covalently bound.

It can be concluded, from the above stated results, that we have formed a γγ-FITC species.

The attachment of FITC to a protein involves a reaction between the isothiocyanate group of FITC and an unprotonated amine side chain, which serves as the nucleophile [20]. At pH = 8 two possible targets are the terminal alpha amino group (pka≈7.0) and the epsilon amino group of lysine (pka≈9.5). A number of mammalian enolases are known to have a blocked (acetylated) amino terminal group [21], rendering them unreactive towards FITC attack. Although the terminal amino group status of γγ is unknown, it is reasonably

Figure 1: Absorption spectra of FITC and γγ-FITC (after the labelling procedure) in buffer A at 25°C.

---- = FITC

—— = γγ-FITC

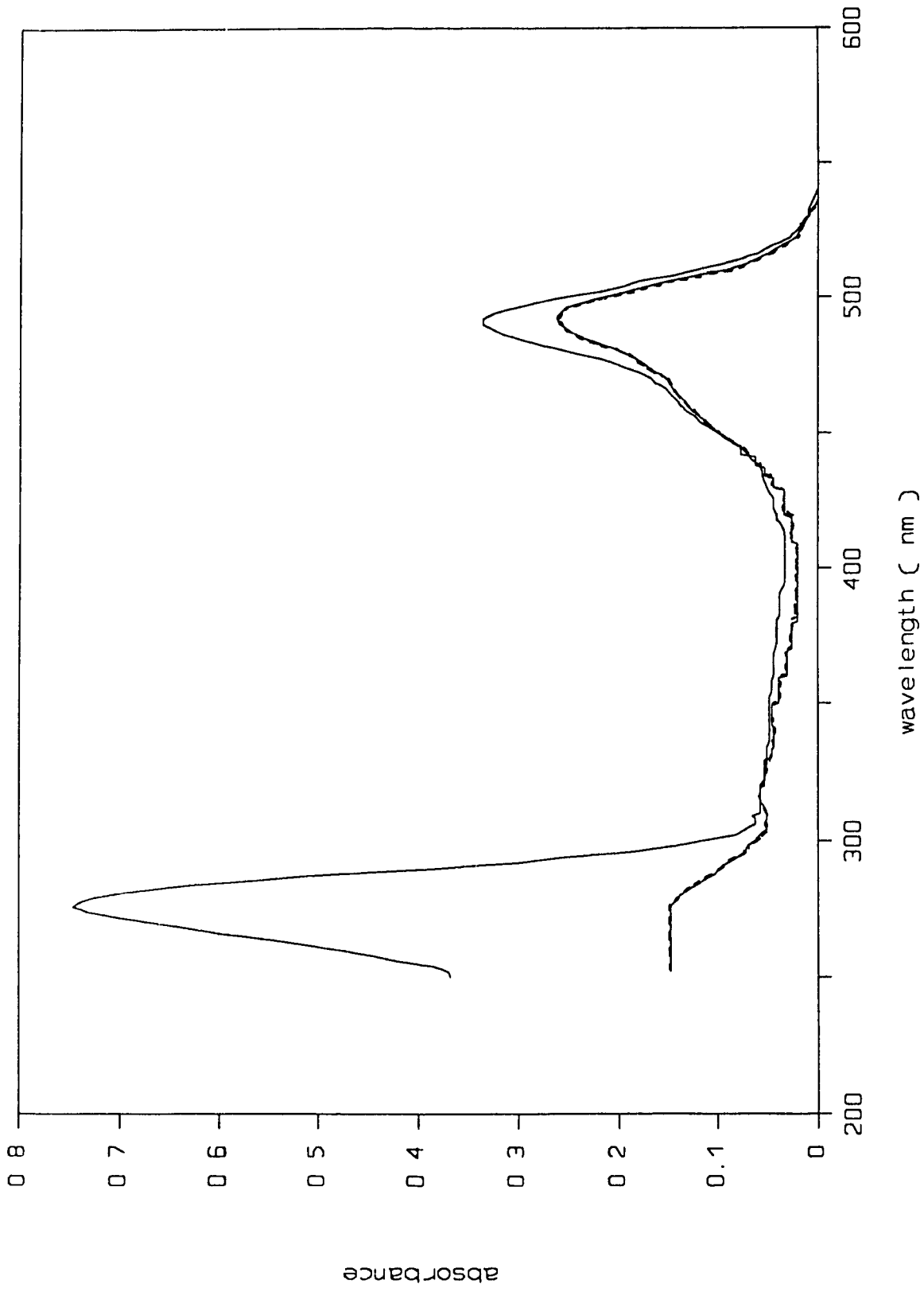
absorbance
0.8
0.7
0.6
0.5
0.4
0.3
0.2
0.1
0
200
300
400
500
600
wavelength (nm)

Figure 2: Excitation emission spectra and polarization of FITC and γγ in buffer A, pH = 7.15 at 25°C.

——= Excitation spectrum of FITC
(emission set at 520nm)

—— = Emission spectrum of FITC.
(excitation set at 492nm)

---- = Excitation spectrum of γγ.
(emission set at 520nm)

---- = Emission spectrum of γγ.
(excitation set at 492nm)

[γγ] = 54nM ; signal gain = 1.5

[FITC] = signal gain of 1.5 (see materials and methods)

For polarization measurements, of the above samples;

Excitation = 492nm

Emission = 520nm

Signal gain ≈ 3.0

G = 0.87

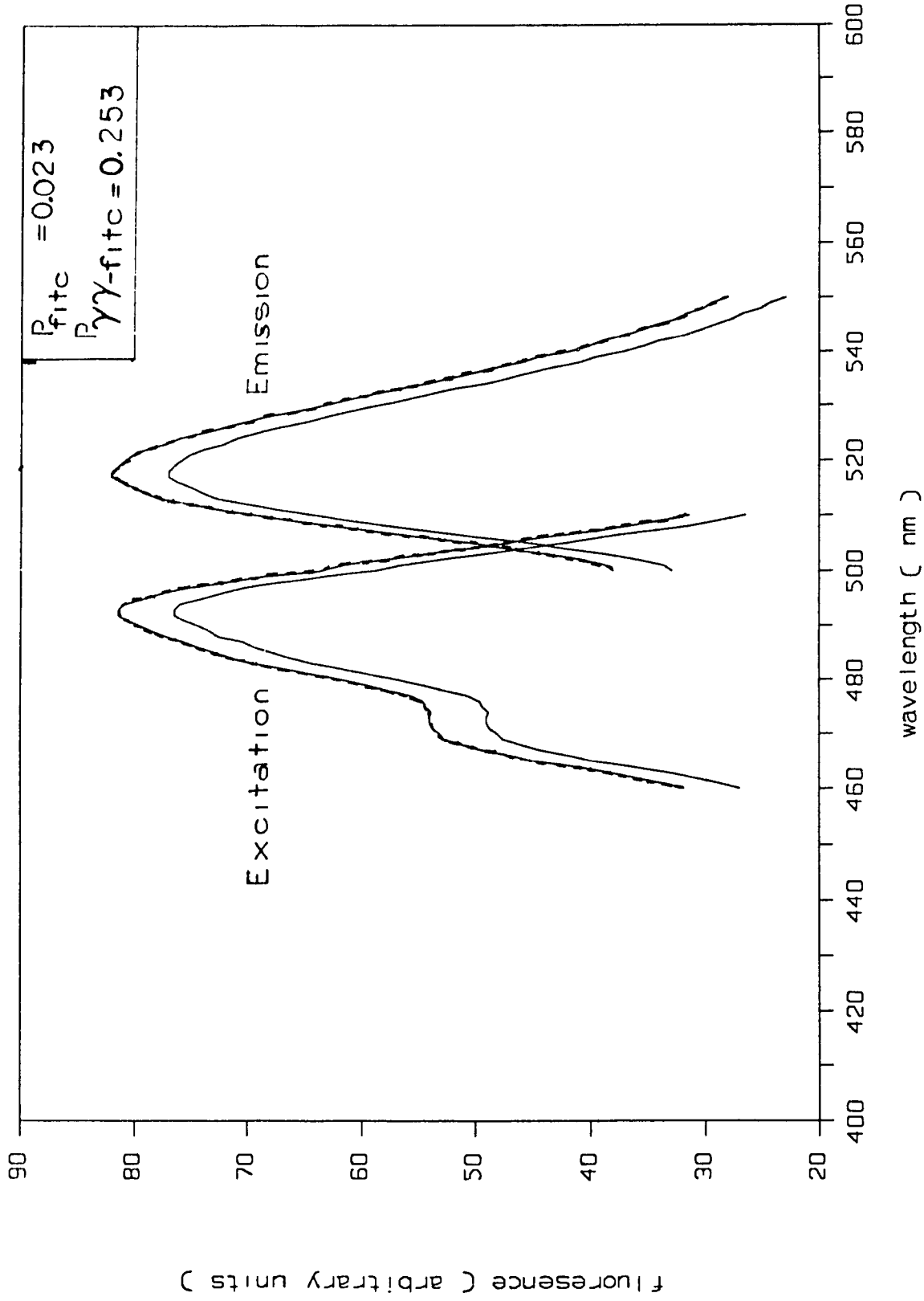
P_{fitc} =0.023
$P_{\gamma\gamma\text{-}fitc}$ =0.253
Emission
Excitation
fluorescence (arbitrary units)
wavelength (nm)
90
80
70
60
50
40
30
20
400
420
440
460
480
500
520
540
560
580
600

assumed that the FITC is covalently bonded to a lysine residue(s).

A:2.0: Degree of labelling of γγ and relative specific activity of γγ-FITC.

Using the absorption of FITC in γγ-FITC at 490nm (fig.1) and an extinction coefficient of 3.4 x 10^4 M^{-1} cm^{-1} [18,19], the degree of labelling was calculated to be 0.87 FITC/dimer. The labelling procedure reproducibly yields a degree of labelling of 0.8-1.0 FITC/dimer.

The specific activity of γγ-FITC is found to be 90-100% that of the native γγ.

A:2.1: Gel filtration of γγ and γγ-FITC.

In order to determine if γγ-FITC remains dimeric, gel filtration was performed. Fig.3A shows the results of the application of γγ and γγ-FITC to a sephacryl S-200 gel permeation column. The elution profile of γγ-FITC, as monitored by activity and fluorescence emission, is identical to γγ. Figure 3B shows that the molecular weight standards and γγ follow the expected log molecular weight linear relationship with elution volume. It is concluded that γγ-FITC remains dimeric. The overlap of the emission elution profile of γγ-FITC with it's activity profile is expected to occur if the FITC is covalently bonded to γγ.

In conclusion then, a γγ-FITC species has been formed which retains identical specific activity and chromatographic behaviour as the native unlabelled

Figure 3A: Elution profile of γγ, γγ-FITC and standard molecular weight markers on sephacryl S-200.

Standard molecular weight markers.

□ = blue dextran (void volume marker)

◇ = bovine serum albumin (BSA) ; 68000 daltons, monitored at OD_{280}

+ = egg albumin ; 45000 daltons monitored at OD_{280}

γγ

△ = γγ ; 91000 daltons monitored via activity (materials and methods)

γγ-FITC

× = γγ-FITC, monitored via activity

▽ = γγ-FITC monitored via emission at 520nm

The OD_{280} values comprising the elution profile of egg albumin and blue dextran are the true experimental values. The observed OD_{280} values of BSA, the activity of γγ and γγ-FITC and the emission of γγ-FITC were numerically normalized to the OD_{280} values of egg albumin.

Column running conditions outlined in materials and methods.

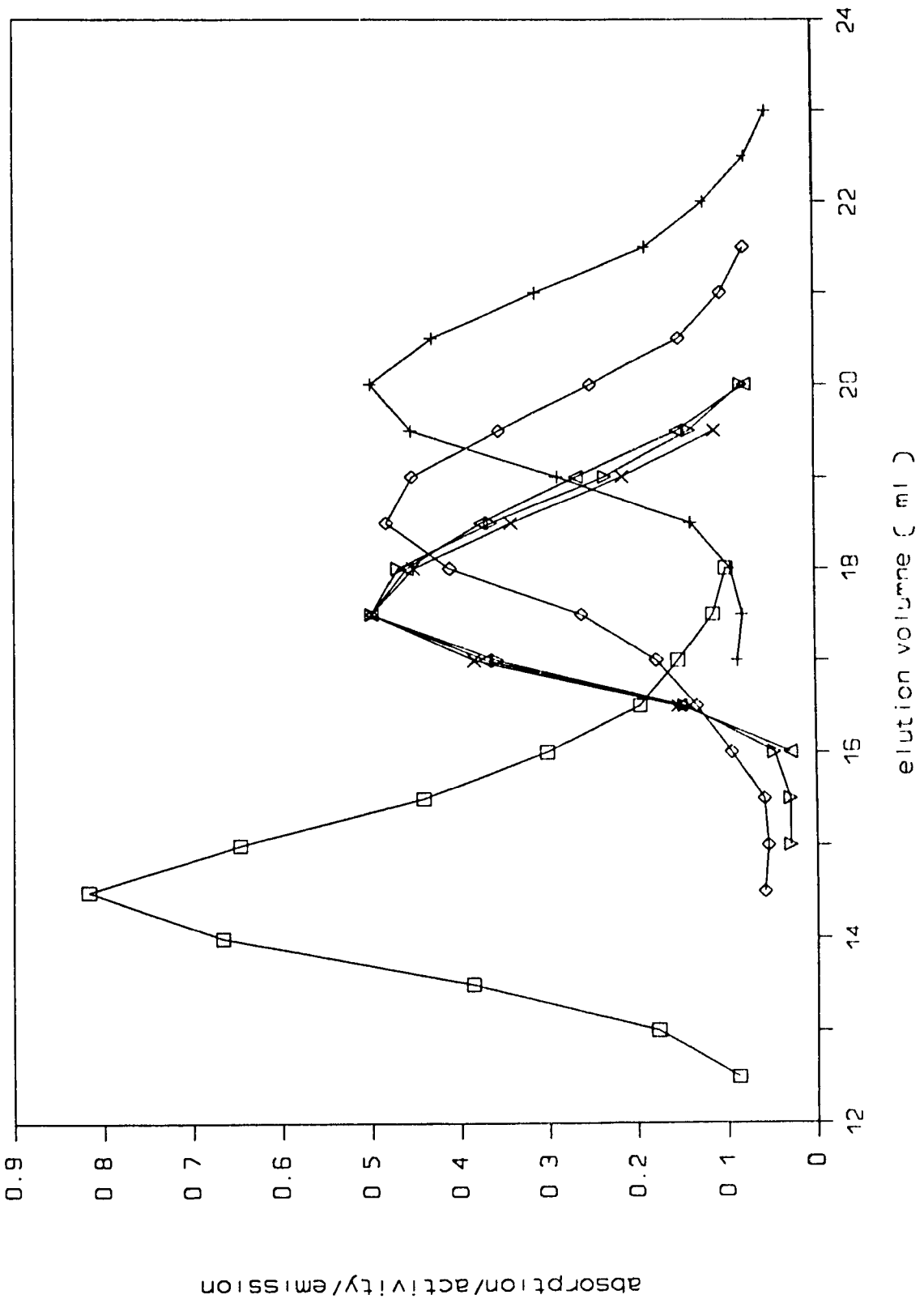
absorption/activity/emission
0.9
0.8
0.7
0.6
0.5
0.4
0.3
0.2
0.1
0
12
14
15
18
20
22
24
elution volume (ml)

Figure 3B: Plot of log molecular weight versus elution volume of γγ and the molecular weight standards used in figure 3A.

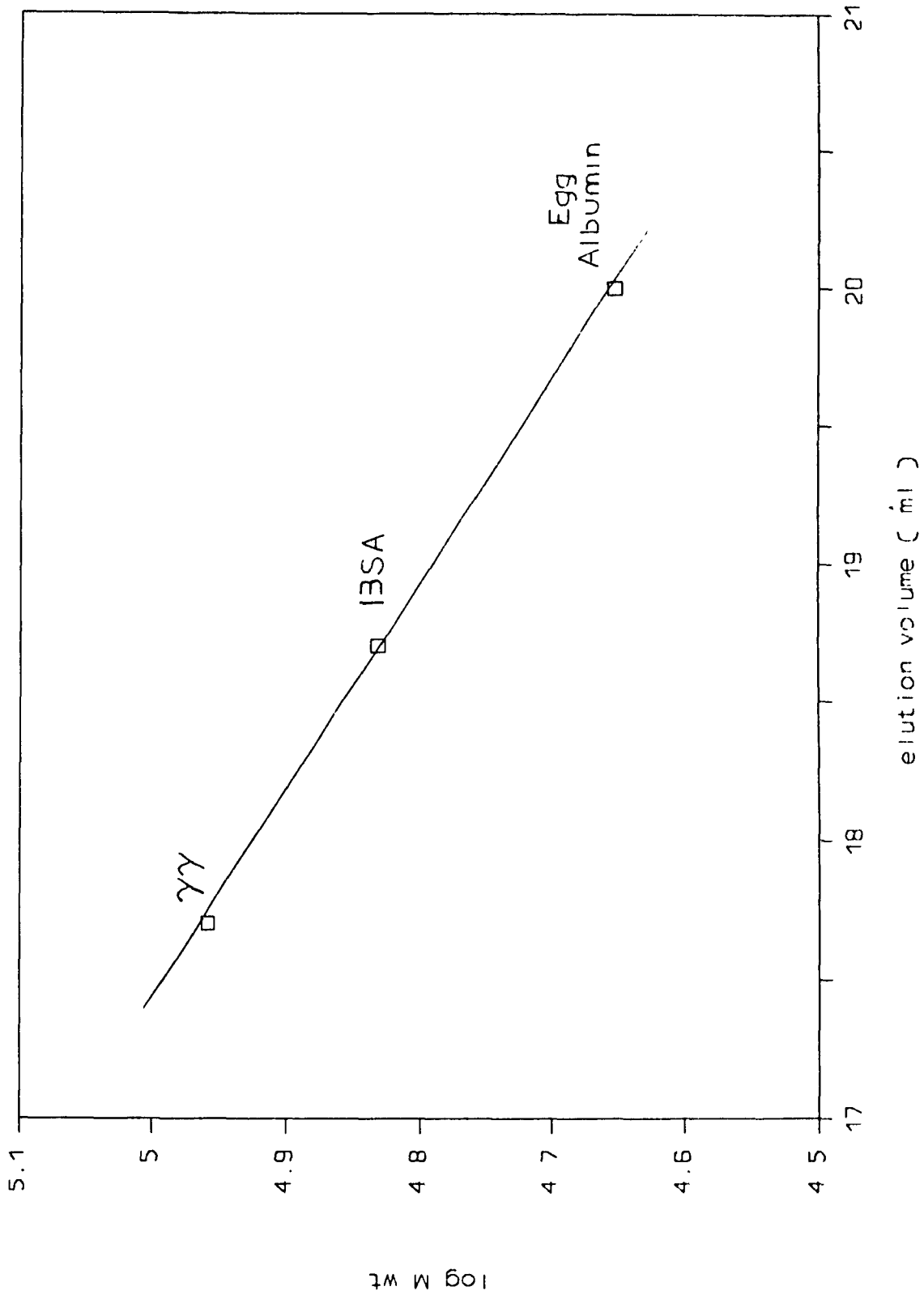
log M wt
5.1
5
4.9
4.8
4.7
4.6
4.5
17
18
19
20
21
elution volume (ml)
γγ
BSA
Egg
Albumin

γγ. Consequently, no measurable perturbation of the native state of γγ is observed upon the covalent attachment of FITC to generate the γγ-FITC species.

B:CHARACTERIZATION OF THE POLARIZATION OF γγ-FITC.

In this section we will characterize γγ-FITC in terms of its observed polarization (P) value of 0.253 ± 0.001 (inset of figure 2). We will initially determine what the theoretical polarization value should be. It will be shown that the observed value is much lower than the theoretical value for FITC attachment to a macromolecule of 91000 daltons. We will then proceed to establish the polarization parameters which account for this deviation from theory. The reader is referred to the appendix for a detailed treatment of the theory of fluorescence polarization/anisotropy.

B:1.0: The Perrin equation in its angular dependent form.

It is not possible to accurately calculate the expected polarization (anisotropy) for γγ-FITC, or any labelled macromolecule, without making assumptions regarding:

(1) The molecular shape of γγ-FITC.

(2) The degree of hydration of γγ-FITC.

(3) The rigidity of FITC attachment to γγ.

and/

(4) The angle between the absorption and emission dipoles of FITC.

The perrin equation (eq.1) [22] of anisotropy theoretically describes the expected anisotropy to be observed for fluorophore attachment to a

macromolecule.

$$A = A_0 (1 + T_f / T_c)^{-1} \qquad \text{(eq.1)}$$

Where: A = anisotropy

A_0 = limiting anisotropy; the A observed when no rotational motion is occurring during the lifetime of the fluorophore.

T_f = fluorescent lifetime (nsec.) of the fluorophore.

T_c = rotational correlation time of the fluorophore; time taken ,in nsec. to rotate about 30 degrees.

Equation 1 can be expanded to its angular dependent form as:

$$A = 2/5 \left(\frac{3 \cos^2 \alpha - 1}{2} \right) \left(\frac{3 \cos^2 R - 1}{2} \right) \qquad \text{(eq.2)}$$

Where; $2/5 \left(\frac{3 \cos^2 \alpha - 1}{2} \right) = A_0$ (eq.3)

α = angle between absorption and emission dipoles of the fluorophore.

R = angle through which the macromolecule rotates during the T_f of the fluorophore.

$$\left(\frac{3 \cos^2 R - 1}{2} \right) = (1 + T_f / Tc)^{-1} \qquad \text{(eq.4)}$$

If the fluorophore is not rigidly attached to the macromolecule, such that it is capable of rotation independent of the macromolecule, then the T_c of the fluorophore will not be equal to the T_c of the macromolecule. The consequence of this, as will be experimentally illustrated shortly, is that the A_0 will be lowered to an apparent limiting anisotropy (A_0') [23].

$$A_0' = A_0 \left(\frac{3 \cos^2 \beta - 1}{2} \right) \qquad \text{(eq.5)}$$

Where; β = angle over which the fluorophore is free to rotate relative to the macromolecule.

Consequently, the perrin equation (eq.1) must be modified to incorporate this fluorophore motion by substitution of eq.5 into eq.1 to yield;

$$A = A_0' \left(\frac{3 \cos^2 R - 1}{2} \right) \qquad \text{(eq.6)}$$

or the angular dependent form;

$$A = 2/5 \left(\frac{3 \cos^2 \alpha - 1}{2} \right) \left(\frac{3 \cos^2 \beta - 1}{2} \right) \left(\frac{3 \cos^2 R - 1}{2} \right) \qquad \text{(eq.7)}$$

B:1.1: Theoretical value of polarization for γγ-FITC.

We can now ask, with the following considerations, what the theoretical anisotropy of γγ-FITC, or any labelled macromolecule, is predicted to be.

(1) If the absorption and emission dipoles are collinear then $\alpha = 0$ and consequently $A_0 = 0.4$

(2) If the FITC is rigidly attached to γγ then $\beta = 0$ and consequently:

$$\frac{3\cos^2\beta - 1}{2} = 1$$

(3) T_c is defined as:

$$T_c = \frac{V\,N}{R\,T} \qquad \text{(eq.8)}$$

Where: V = volume of sphere

(m^3 $mole^{-1}$)

N = viscosity of solvent

(Kg m^{-1} sec^{-1})

R = Gas constant

(J K^{-1} mol^{-1})

T = temperature

(K)

The expression theoretically states the rotational time (sec) of a sphere in solution. It does not take into account any degree of hydration and, therefore, holds only for an anhydrous sphere. The equation, as such, must be modified if it is to predict the T_c of a protein. This was done by measuring the hydrated molecular volume (V_h) of a number of proteins and relating it to their molecular weight (M). Typically the hydrated specific volume (v + h) was 1 cm^3 $gram^{-1}$ [22]. The equation could then be restated as:

$$Tc = \frac{M\,N}{R\,T}(v + h) \qquad \text{(eq.9)}$$

Where; $M(v + h) = V_h$

It is to be noted that, in effect, what has been done here is to add on an extra volume, due to hydration, to a sphere. Equation 9, then, tells us the expected T_c of a hydrated spherical protein from a simple knowledge of its molecular weight. The predicted T_c is now about 12% [23] greater than the T_c predicted for an anhydrous sphere (i.e. larger spheres rotate faster than smaller ones). Equation 9, however, does not take into account the shape of the protein and, as such, is oblivious to the fact that a nonspherical protein, although possibly having the same V_h as a spherical protein, will rotate more slowly than a spherical protein. The equation also does not encompass the larger effective solvation shell for rotation than for hydration. These shortcomings of equation 9 are proposed to account for the fact that the experimentally observed T_c of a

protein (from time resolved anisotropy decay curves) is generally twice that which is predicted for an anhydrous sphere [23].

Using equation 9 the theoretical T_c for γγ (91000 g $mole^{-1}$) at 25°C is 32.8 nsec. This value could, in actuality, then, be up to ≈ 60 nsec but not below 32.8 nsec.

(4) The T_f of FITC in γγ-FITC was experimentally measured (fig.4) and was found to be 3.9 ± 0.1 nsec (see materials and methods).

Using eqs. 7 and 4 and the above considerations we have;

$A_{theoretical}$ = (0.4) (1) (1) (T_c =32.8) = 0.358

$A_{theoretical}$ = (0.4) (1) (1) (T_c =60) = 0.376

therefore;

$A_{theoretical}$ = 0.367 ± 0.009

or/

$P_{theoretical}$ = 0.465 ± 0.01

P is calculated from A using the following relationship:

$$P = \frac{3A}{2 + A} \qquad \text{(eq.10)}$$

In other words, if γγ-FITC, involved rigid attachment of FITC, and had collinear absorption and emission dipoles, the P value at 25°c would be expected to be 0.465 ± 0.01. This is to be contrasted with the observed value of

Figure 4: Fluorescent emission decay for γγ-FITC.

Solvent = Buffer A, pH = 7.15

[γγ-FITC] = 1 μM

Excitation = 355 nm

Emission = 520 nm

Signal gain = 5

Fluorescent lifetime = 3.9 ± 0.1 nsec.(see materials and methods).

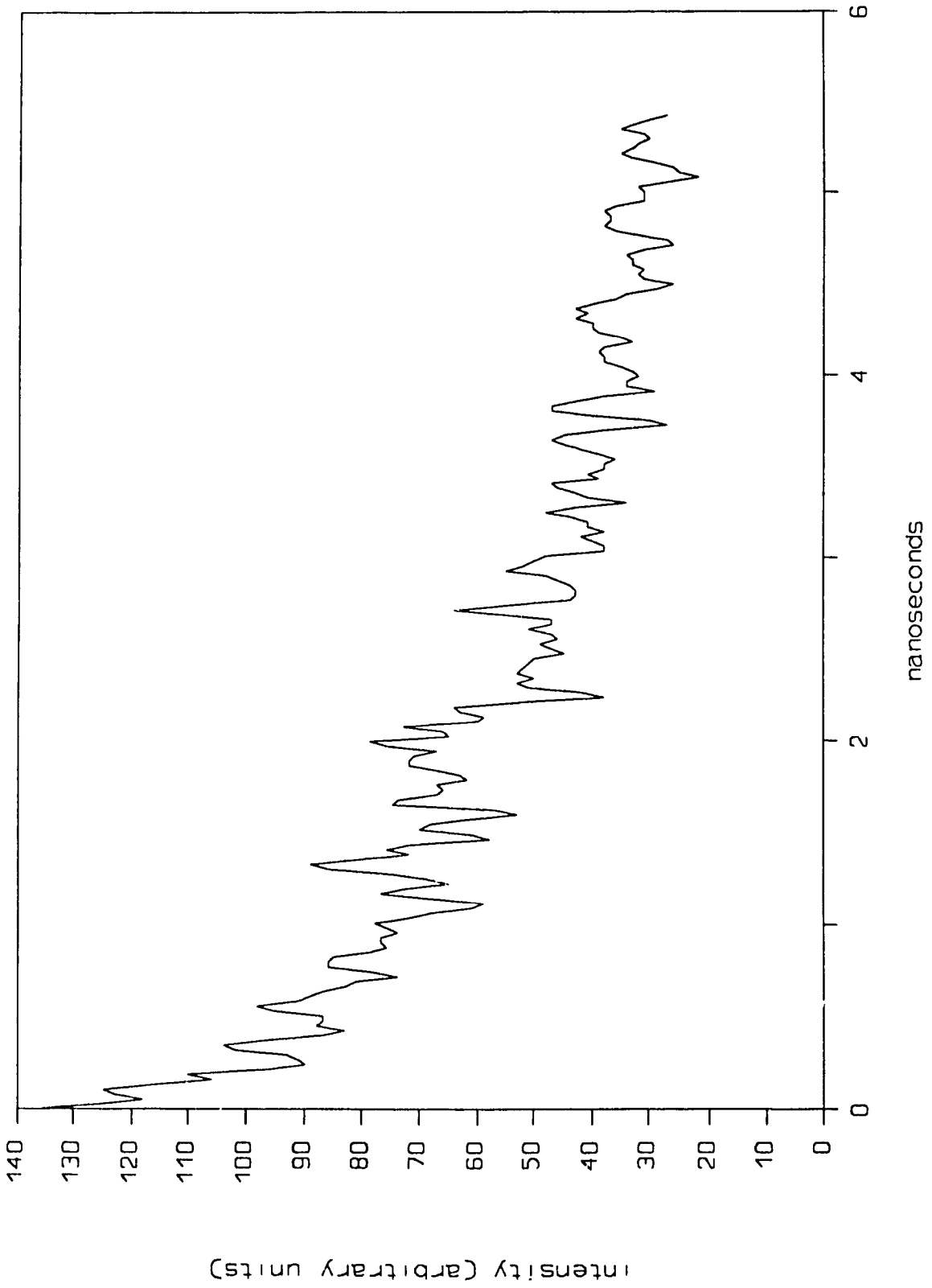
intensity (arbitrary units)
0
10
20
30
40
50
60
70
80
90
100
110
120
130
140
0
2
4
6
nanoseconds

0.253 ± 0.001 (inset of fig.2). The question then is why is the observed P value much less than the theoretical.

B:1.2: Observation of noncollinear dipoles and nonrigid attachment of FITC to γγ.

To observe whether there is nonrigid attachment of FITC and/or whether the absorption and emission dipoles of FITC are collinear we will construct a plot of P versus viscosity. The usefulness of this plot will become evident through the following manipulation.

Equation 1 can be stated in terms of polarization as:

$$(P - 1/3) = (P_0 - 1/3)\ (1 + T_f/T_c) - 1 \qquad \text{(eq.11)}$$

Taking the reciprocal of equation 11 we obtain;

$$(1/P - 1/3) = (1/P_0 - 1/3)\ (1 + T_f / T_c) \qquad \text{(eq.12)}$$

Substitution of equation 9 into equation 12 gives;

$$(1/P - 1/3) = (1/P_0 - 1/3)\quad 1 + \left(\frac{T_f\ R\ T}{V_h\ N} \right) \qquad \text{(eq.13)}$$

Expanding, factoring and rearranging gives (eq. 14);

$$(1/P - 1/3) = (1/P_0 - 1/3) + (1/P_0 - 1/3)\left(\frac{T_f R}{V_h}\right)\left(\frac{T}{N}\right) \qquad \text{(eq.14)}$$

Equation 14 is to be recognized as the linear relationship;

$$Y=mx+b.$$

Consequently, a plot of $1/P - 1/3$ versus T/N, obtained by measuring P as a function of viscosity, will be linear with an intercept of $1/P_0 - 1/3$ and a slope of $1/P_0 - 1/3 \frac{T_f R}{V_h}$. It is to be recalled that this relationship holds only for a molecule of FITC rigidly attached to $\gamma\gamma$.

The theoretical plot for $\gamma\gamma$-FITC (fig.5), which assumes α and $\beta = 0$, illustrates that as the viscosity is increased the viscous drag on $\gamma\gamma$-FITC increases, which increases the T_c for $\gamma\gamma$-FITC and therefore increases the polarization. At infinitely high viscosity ($T/N = 0$) no rotational motion occurs and since α and β are 0, then the intercept on the $1/P_0 - 1/3$ axis gives a P_0 of 0.5. In this case then, there is only one T_c upon which the viscosity is acting and consequently the plot is linear.

Figure 6 shows the experimental plot of polarization versus viscosity for FITC. A linear relationship is, again, expected owing to the sole T_c upon which the viscosity is acting. P_0, from the $1/P - 1/3$ intercept, is found to be 0.397 $\pm$ 0.028. This is in contrast to the theoretical value of 0.5. The significance of this will be discussed shortly.

Figure 5: Theoretical plot of polarization versus viscosity for γγ-FITC.

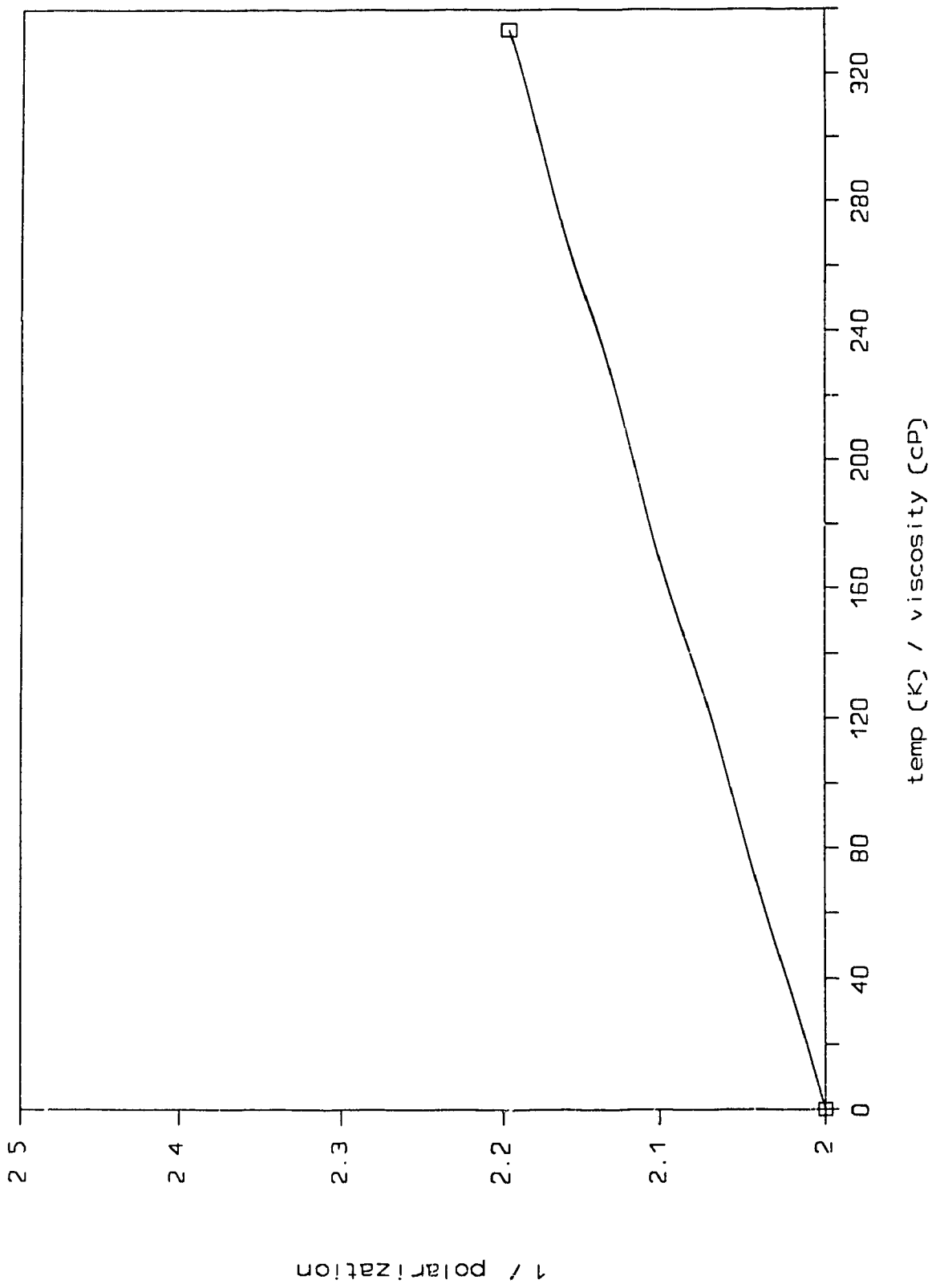
1 / polarization
2.5
2.4
2.3
2.2
2.1
2
0
40
80
120
160
200
240
280
320
temp (K) / viscosity (cP)

Figure 6: Polarization versus viscosity for FITC.

Temperature = 298.15 K

[FITC] = 75 nM

Excitation = 492 nm

Emission = 520 nm

$1 / P_0 = 2.53 \pm 0.18$

Experimental protocol as per materials and methods.

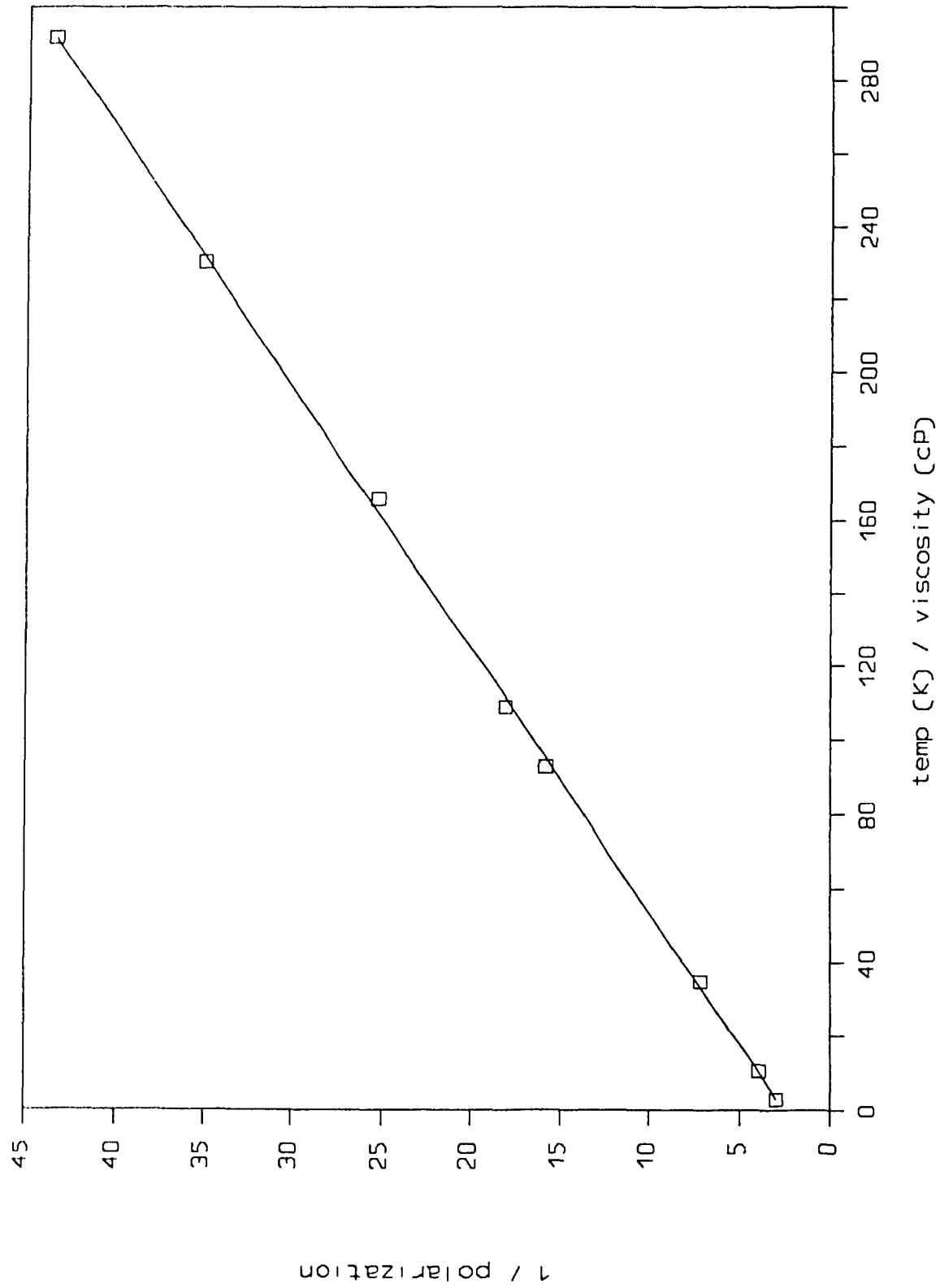
1 / polarization
0
5
10
15
20
25
30
35
40
45
0
40
80
120
160
200
240
280
temp (K) / viscosity (cP)

The plot of γγ-FITC (fig.7) is nonlinear. Included in figure 7 are the plots for FITC (fig.6) and the theoretical γγ-FITC (fig.5). The non-linearity, throughout the viscosity range, is indicative of nonrigid attachment of FITC to γγ and arises because we are now dealing with at least two values of T_c. One for γγ and one for the free rotation of FITC relative to γγ. At lower viscosities, (≈ 340 to 200 K/N in figure 7) a linearity is observed, but at higher viscosities (greater than 200 K/N), γγ, due to it's much larger V_h, will be subjected to the increased viscous drag of the solvent to a much greater degree than the free rotation of FITC and consequently, a deviation from linearity is observed.

Both FITC and γγ-FITC are shown to intersect the 1 / P - 1/3 axis at the same point yielding a $P_0 = 0.397 \pm 0.028$. This is so, because at T/N = 0 there is no rotational motion of γγ and FITC and, as such, the angular terms α and β collapse to yield; $P = P_0$ (or $A = A_0$).

It is to be recalled from equation 3 that when α is equal to 0 that A_0 is 0.4 (or $P_0 = 0.5$). The observed value of 0.397 ± 0.028 for P_0 is then due only to photoselection (see appendix) and some intrinsic angle between the absorption and emission dipoles of FITC.

The results of figure 7, therefore, enable us to qualitatively state;

(1) The FITC is not rigidly attached to γγ and is therefore capable of some degree of rotation relative to γγ (i.e. β is not equal to 0).

As was stated in section A (1.0), we can assume that the FITC is specific for lysine residues on the enolase dimer, however, due to the absence of

Figure 7: Polarization versus viscosity for γγ-FITC, γγ $FITC_{theoretical}$ and FITC.

$\cup$ = FITC (as in fig.6)

$+$ = γγ-$FITC_{theoretical}$ (as in fig.5)

$\square$ = γγ-FITC

Temperature = 298.15 K

Excitation = 492 nm

Emission = 520 nm

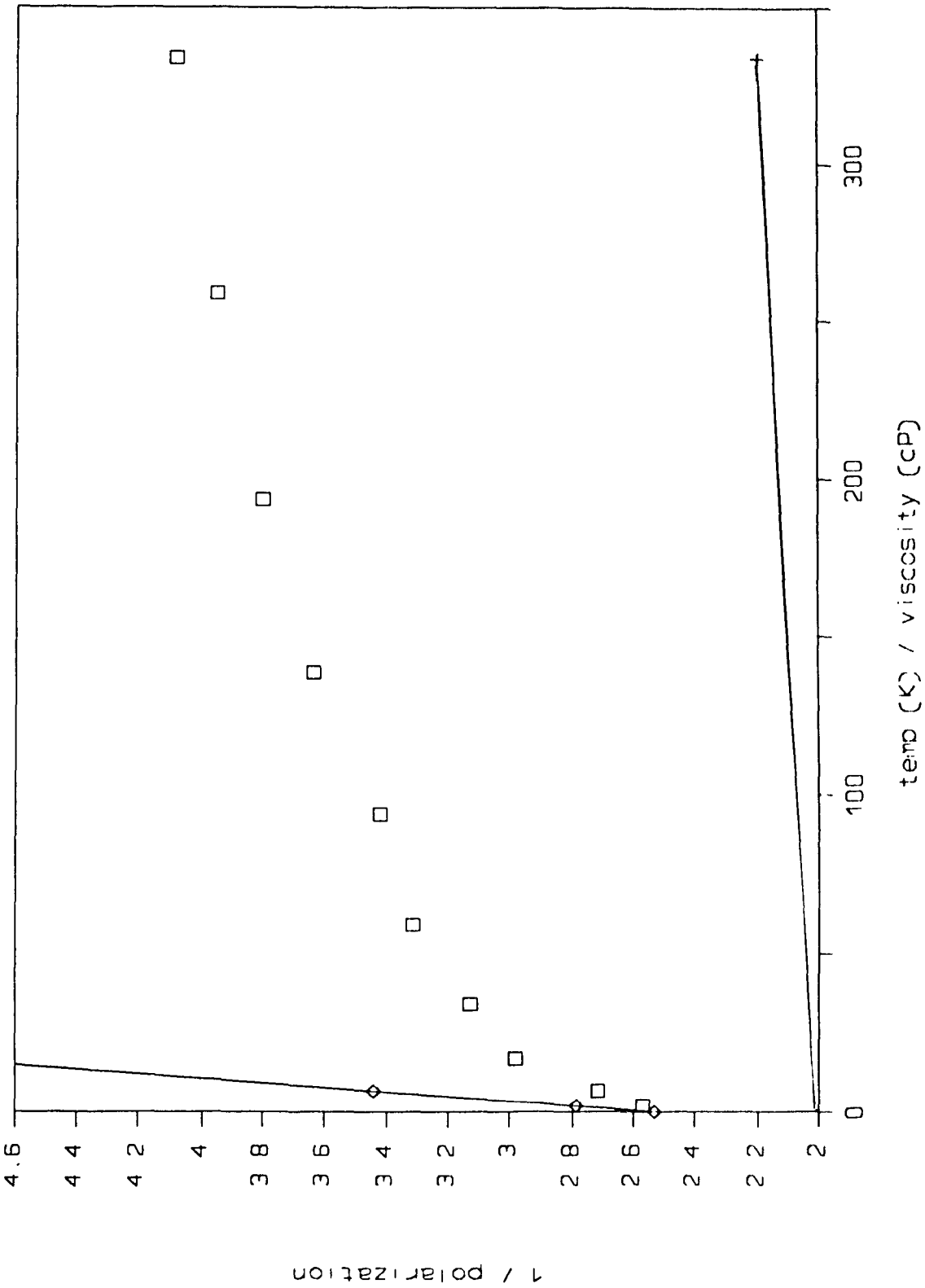
1 / polarization
4.6
4.4
4.2
4
3.8
3.6
3.4
3.2
3
2.8
2.6
2.4
2.2
2
0
100
200
300
temp (K) / viscosity (cP)

sequence information on the labelled dimer we cannot differentiate between labelling at a specific lysine residue (with a low pKa) or nonspecific labelling of a number of lysine residues. Consequently, when we speak of " The FITC " being capable of some degree of rotation relative to $\gamma\gamma$, this is taken to be inclusive of the possibility that the degree of rotation observed may be an average of a number of rotational motions.

and/

(2) The absorption and emission dipoles of FITC are not collinear (i.e. α is not equal to 0). This implies that either there is an intrinsic angle between the absorption and emission dipole or that excitation at 492 nm yields various excited state species, due to overlapping electronic transitions, which are not collinear with the emission dipole. This will be discussed later (section D) where the latter case will be shown to be valid.

In any case, the consequence of the above is that we observe a lower P value for $\gamma\gamma$-FITC than is theoretically expected.

B.1.3: Calculation of α and β.

With the use of the A_0 definition in equation 3, and equation 5 we can provide estimates of the values of α and β.

Using equation 3 and $P_0 = 0.397 \pm 0.028$ (or $A_0 = 0.306 \pm 0.025$), α is calculated to be 23.14 ± 3.3 degrees. In other words there is an angle of 23.14

± 3.3 degrees between the absorption and emission dipoles of FITC in γγ-FITC.

To calculate β, using equation 5, we will need an estimate of A_0'.Extrapolation of the linear portion of the plot of polarization versus viscosity for γγ-FITC (fig. 7) to T/N = 0 yields an apparent limiting polarization (P_0') of 0.299 ± 0.004 (fig. 8). Conversion of this value into anisotropy , using equation 8, gives A_0' = 0.222 ± 0.003. The difference between A_0' (0.222 ± 0.003) and A_0 (0.306 ± 0.025), or P_0' (0.299 ± 0.004) and P_0 (0.397 ± 0.028), then, represents the freedom of FITC motion relative to γγ. By the use of equation 5, β is calculated to be 24.9 ± 3.5 degrees.

B.1.4: Theoretical polarization of γγ-FITC with nonzero values of α and β.

Since we now have experimental values for α and β and a theoretical estimate of R, we can ask what the theoretical polarization would be if;

α = 23.14 ± 3.3 degrees T_c = 32.92 - 60 nsec.

β = 24.87 ± 3.5 degrees T_f = 3.9 ± 0.1 nsec.

Using equations 7 and 4 we have:

$$A_{theoretical} = 0.208 \pm 0.041$$

or/

$$P_{theoretical} = 0.281 \pm 0.051$$

Figure 8: Extrapolation of the linear portion of figure 7 (γγ-FITC) to infinite viscosity to obtain P_0'.

■ = regressed data points

—— = regressed line

1/P intercept = $1/P_0' = 3.34 \pm 0.04$

$P_0' = 0.299 \pm 0.004$

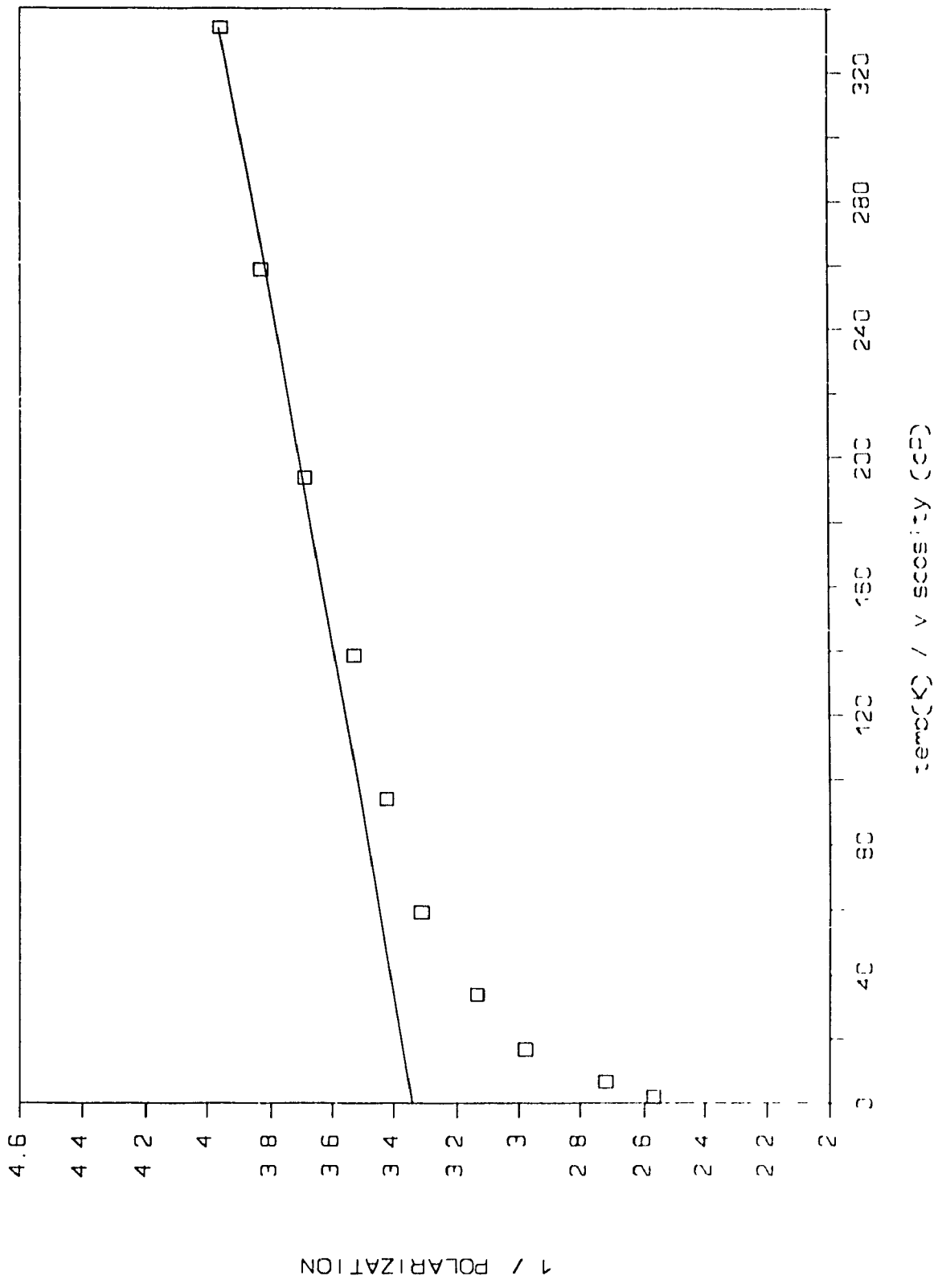
1 / POLARIZATION
4.6
4.4
4.2
4
3.8
3.6
3.4
3.2
3
2.8
2.6
2.4
2.2
2
0
40
80
120
160
200
240
280
320
temp(K) / susceptibility (cgs)

Since the observed polarization of 0.253 ± 0.001 (inset of fig 2) is in good agreement with the theoretical it is concluded that the low observed polarization value, relative to the theoretical value of 0.465 ± 0.01 (which assumes α and β = 0, B.1.1), can be accounted for through noncollinear dipoles and nonrigid attachment of FITC to $\gamma\gamma$.

C: EFFECT OF DISSOCIATION UPON THE POLARIZATION OF γγ-FITC.

In the preceding section we showed that the observed polarization (anisotropy) of γγ-FITC could be explained in terms of equation 7. For dissociation the following theoretical scheme is applicable;

$$A_{dimer} = 2/5 \left(\frac{3\cos^2\alpha_{(D)}-1}{2} \right)\left(1 + \frac{T_{f(D)}}{T_{c(D)}}\right)\left(\frac{3\cos^2\beta_{(D)}-1}{2}\right) \quad \text{(eq.14)}$$

DISSOCIATION

$$A_{monomer} = 2/5 \left(\frac{3\cos^2\alpha_{(M)}-1}{2} \right)\left(1 + \frac{T_{f(M)}}{T_{c(M)}}\right)\left(\frac{3\cos^2\beta_{(M)}-1}{2}\right) \quad \text{(eq.15)}$$

Where: $_{(D)}$ = dimer

$_{(M)}$ = monomer

Briefly and in the simplest case, a decrease in polarization upon dissociation of γγ-FITC is expected due to a lower T_c for the monomer than the dimer which results in the further depolarization of the light, during the fluorescent lifetime of FITC, relative to the dimer. In other terms;

$$\text{Since } T_{c(M)} < T_{c(D)} \text{ ; Therefore } A_M < A_M$$

Since this is the simplest case we then assume that;

(1) $\alpha_{(M)} = \alpha_{(D)}$

(2) $\beta_{(M)} = \alpha_{(D)}$

and/

(3) $T_{f(M)} = T_{f(D)}$

The purpose of this section is to, firstly, find a condition which will promote the dissociation of γγ-FITC and, secondly, to observe any change in polarization upon dissociation. It will be shown that in the presence of 0.5 M $NaClO_4$, γγ-FITC is dissociated and is accompanied by an ≈ 15% decrease in polarization.

C.1: Dissociation of γγ-FITC.

C.1.1: Choosing the dissociating agent.

Dissociation of oligomeric proteins can be accomplished using a number of techniques [24]. These include:

(1) Chemical denaturants.

(2) pH variation [25].

(3) Dilution [10].

(4) Ligand effects [26].

(5) Temperature [27].

(6) Pressure [12].

Temperature and pH variation experiments as methods of dissociation of mammalian enolases have not been conducted and $\gamma\gamma$, as previously mentioned (see introduction) has been shown to not undergo dissociation upon dilution.

Ligand effects, such as the ATP-dependent dissociation of glyceraldehyde-3-phosphate dehydrogenase, [26] are highly dependent upon the protein under study. No such ligand effects have been found for $\gamma\gamma$.

The use of chemical denaturants (includes electrolytes, ureas, and guanidinium hydrochloride) are independent of the protein under study. The only variables being the concentration and identity of the chemical denaturant needed for dissociation, which in turn depends upon the particular subunit interactions of the protein.

The term "chemical denaturants" is misleading since it implies denaturation and consequently tertiary structural loss. This may be expected when using urea and guanidinium hydrochloride since these substances act through a stabilization of the hydrophobic interactions between nonpolar groups and water, and by increasing the affinity of the solvent for amide and peptide groups [28]. In fact all of the constituent groups of a protein are more soluble in urea solutions than they are in water [28].

Electrolytes (Cl^-, Br^-, I^-, ClO_4^-, SCN^-, etc.) can also generate denatured proteins but in many cases, discrete steps of dissociation and denaturation are observed [24], with dissociation occurring at low electrolyte concentrations and

denaturation occurring at high concentrations. Electrolytes are thought to alter the native conformation of proteins by producing changes in the water structure solvating the protein (i.e. act as chaotropic ions by favouring the transfer of apolar groups to water) and by preferential interaction with the protein constituents [29]. (i.e. preferential binding to the dissociated species possibly resulting from the availability of extra binding sites).

The question, then, is which electrolyte shall we use to instigate dissociation of γγ-FITC. Two general criteria must be met:

(1) The electrolyte (salt) should not effect the fluorescent lifetime of FITC on γγ-FITC.

If the dissociating agent, itself, quenches the T_f of FITC (i.e. $T_{f(M)} < T_{f(D)}$) then, although the monomer is depolarizing the light to a greater degree than the dimer, our window to this event is shorter and as such the observational consequence would be a smaller change in polarization than if quenching was not occurring (eqs.14 and 15). Depending upon the degree of quenching one will decide to use or not use a particular salt. This is so because one could always opt to correct for the quenching. It is of course desirable to have a "silent" dissociating salt.

(2) The salt must completely dissociate γγ-FITC.

During the isolation of mammalian enolases, in our laboratory, the isozymes are dissociated using NaI or KI and NaSCN or KSCN. Both I^- and

SCN^- are, however, effective quenchers of excited state fluorophores.

$NaClO_4$, on the other hand, has not only been shown to be an effective protein dissociating agent at ≤ 0.5 Molar, yielding "correctly" structured monomers [30,31,32,33], but is also not a quencher of the T_f of FITC on γγ-FITC. Figure 9 shows the emission decay of γγ-FITC in $NaClO_4$ (0.5 M). A lifetime of 3.8 ± 0.1 nsec. is observed. It is to be recalled that the fluorescent lifetime of γγ-FITC in the absence of $NaClO_4$ (fig.4) is 3.9 ± 0.1 nsec.

The next step, then, is to establish the concentration of $NaClO_4$ that will be required for dissociation.

C.1.2: Dissociation of γγ as monitored by sodium dodecylsulphate polyacrylamide gel electrophoresis (SDS-PAGE) and chemical cross-linking.

Dissociation of γγ can be visualized using the technique of SDS-PAGE [16] crosslinking. The procedure is covered in materials and methods, however a brief explanation follows.

The experiment involves the incubation of γγ with $NaClO_4$. The bifunctional crosslinking agent glutaraldehyde is added and will covalently link any dimer present through lysine residues on adjacent monomer subunits. The chance of linking two dissociated monomers is assumed to be negligible. The above mixture is then applied to a SDS-PAGE apparatus. The SDS denatures and imparts a large negative charge to the protein which then migrates towards

Figure 9: Fluorescent emission decay for γγ-FITC in $NaClO_4$ (0.5M).

Solvent = Buffer A + 0.5 M $NaClO_4$, pH = 7.15

[γγ-FITC] ≈ 1 μM

Excitation = 355 nm

Emission = 520 nm

Signal gain = 5

Fluorescent lifetime = 3.8 ± 0.1 nsec.(materials and methods).

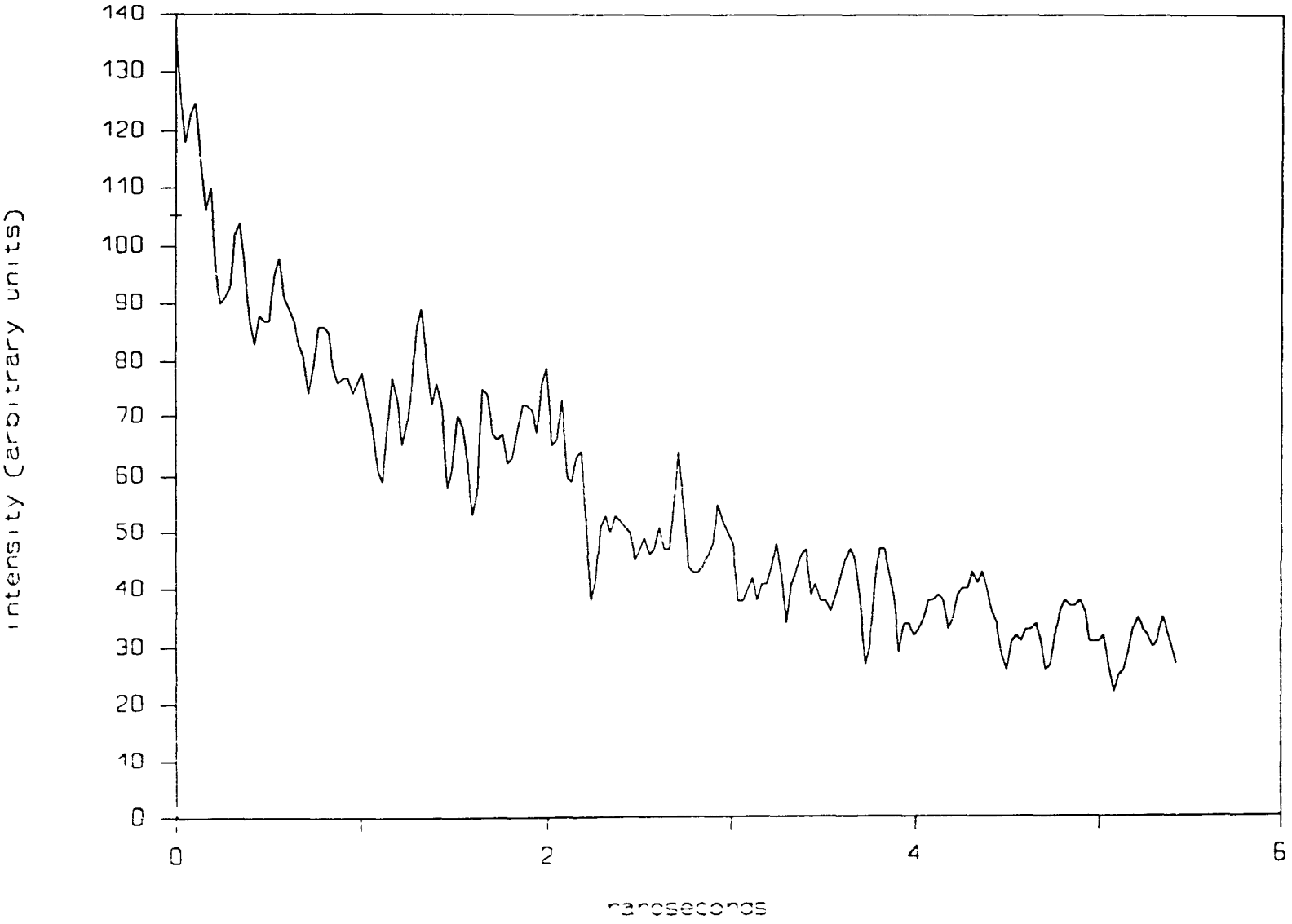
Intensity (arbitrary units)
140
130
120
110
100
90
80
70
60
50
40
30
20
10
0
0
2
4
6
nanoseconds

the anode of the apparatus as a function of its molecular weight. Due to the internal cross-linking of the subunits by glutaraldehyde, denaturation by SDS will not dissociate the cross-linked dimers and consequently the denatured dimers will migrate through the gel separately from the uncrosslinked and denatured monomers.

Subsequent to the experiment the protein is visualized using a coomassie brilliant blue protein stain.

Figure 10 shows the time course of γγ dissociation in 0.6 M $NaClO_4$ in which the glutaraldehyde was added to an aliquot of this mixture at various time intervals. Lanes 1,3,5 and 7 represent the γγ sample, in the absence of $NaClO_4$ at the time intervals specified. It is to be noted that these lanes should consist of only the dimer band(D). The efficiency, however, of crosslinking is not 100% and, as such, not all of the dimers are crosslinked resulting, upon SDS treatment, in the denaturation and dissociation of these uncrosslinked dimers which subsequently migrate as monomers(M). In any case it can be observed that the equilibrium state remains unchanged throughout the experimental time course of two hours. Lanes 2,4,6 and 8 represent the time course in the presence of $NaClO_4$. After 30 minutes of $NaClO_4$ incubation no dimer band is to be observed (lane 4). In the short time interval (less than 1 minute) between the $NaClO_4$ addition to γγ and the subsequent removal of an aliquot to which glutaraldehyde is added, we observe a substantial amount of dissociation (lane 2). Consequently it can be said that 0.6 M $NaClO_4$ dissociates γγ in much

Figure 10: Time course of the dissociation of γγ-FITC in $NaClO_4$ (0.6 M) as monitored by SDS-PAGE crosslinking.

1 = 0 minutes (no salt) 2 = 0 minutes (+ salt)

3 = 30 minutes (no salt) 4 = 30 minutes (+salt)

5 = 60 minutes (no salt) 6 = 60 minutes (+salt)

7 = 120 minutes (no salt) 8 = 120 minutes (+salt)

10 = 120 minutes after salt removal

D = dimer band

M = monomer band

[γγ] incubated with $NaClO_4$ ≈ 1.5 μM

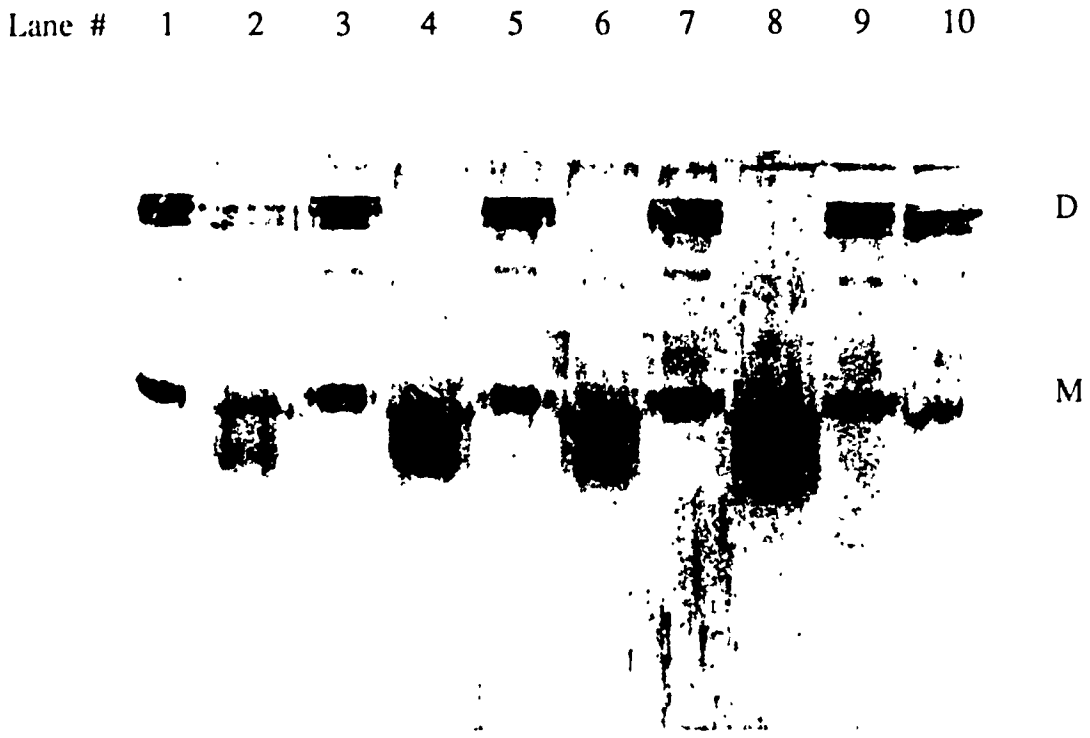
Lane # 1 2 3 4 5 6 7 8 9 10
D
M

less than 30 minutes.

Upon removal of the perchlorate as the insoluble $KClO_4$ by the addition of KCl we observe the reappearance of the dimeric γγ band (lane 10) which then indicates that the dissociation is reversible.

Now, since the crosslinking efficiency is less than 100% we cannot conclude from the data in figure 9 that the dissociation is complete. As well, since both glutaraldehyde and FITC are selective for lysine residues, γγ-FITC was not used for the SDS-PAGE crosslinking studies and therefore, the data do not establish whether γγ-FITC is also dissociated in 0.6 M $NaClO_4$. Gel filtration of γγ and γγ-FITC was consequently run to answer these questions as well as to confirm the SDS-PAGE crosslinking results.

C.1.3: Gel filtration of γγ and γγ-FITC in the presence of 0.6 M $NaClO_4$.

Since the molecular weight of both the γ and γ-FITC monomers is 45000 daltons then if γγ and γγ-FITC both elute at a molecular weight of 45000 daltons this would strongly suggest that both γγ and γγ-FITC undergo complete dissociation in 0.6 M NaClO4.

Figure 11 shows the elution profile of egg albumin (45000 daltons) γγ and γγ-FITC in 0.6 M $NaClO_4$. Both γγ and γγ-FITC are shown to overlap the elution profile of egg albumin. This is taken as strong evidence for the complete dissociation of γγ and γγ-FITC in 0.6 M $NaClO_4$.

The next step, then, is to see if γγ-FITC is capable of probing

Figure 11: Elution profile of γγ and γγ-FITC on a S-200 gel filtration column in the presence of 0.6 M $NaClO_4$.

$[\gamma\gamma]_{applied} \approx 2.0\ \mu M$

$[\gamma\gamma\text{-FITC}]_{applied} \approx 2.0\ \mu M$

= Egg albumin ; 45000 daltons monitered at OD_{280}

= Blue dextran (void volume marker)

= γγ ; monitered via activity (materials and methods; p.18)

= γγ-FITC; monitered via emission 520 nm

Column running conditions outlined in materials and methods

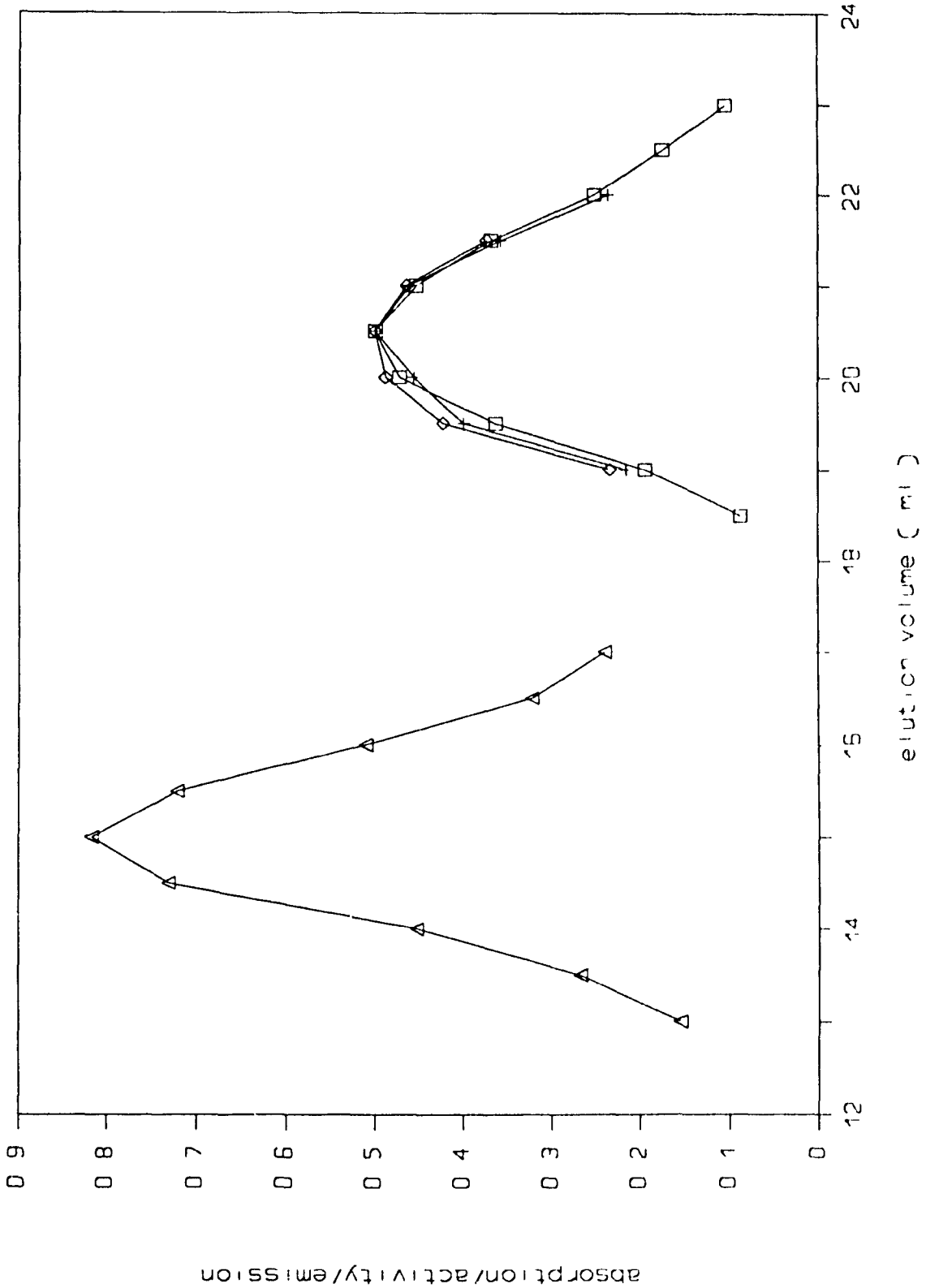
absorption/activity/emission
0.9
0.8
0.7
0.6
0.5
0.4
0.3
0.2
0.1
0
12
14
16
18
20
22
24
elution volume (ml)

dissociation. In other words, does the polarization of γγ-FITC decrease upon salt induced dissociation.

C.2: Polarization of γγ-FITC in $NaClO_4$

C.2.1: Polarization of γγ-FITC in $NaClO_4$ as a function of time.

Figure 12 shows the polarization observed at various time intervals as a function of the $NaClO_4$ concentration. A finite time of 2-3 minutes is required to make a polarization measurement and therefore for 0.1 to 0.5 M $NaClO_4$ the polarization values from 0 to 5 minutes are extrapolated to the value characteristic of γγ-FITC in the absence of NaClO4. For each concentration of $NaClO_4$, we observe the attainment of equilibrium polarization values within 10-15 minutes.

The equilibrium polarization values are replotted as a function of the $NaClO_4$ concentration in figure 13 (line 1). Owing to the small difference between the polarization values observed at 0.4 and 0.5 M $NaClO_4$ we can conclude that the effect of $NaClO_4$ upon the polarization of γγ-FITC has reached completion by 0.5 M $NaClO_4$.

Since the SDS-PAGE crosslinking results (figure 10) and the gel filtration results (figure 11) both provide evidence for the complete dissociation of γγ-FITC in $NaClO_4$, we can conclude that the decreasing polarization in increasing $NaClO_4$ is at least partially if not entirely a result of dissociation (fig.13). Since a plateau of polarization is reached (fig.13) it is also concluded that the

Figure 12: Polarization of γγ-FITC as a function of time in 0 - 0.5 M $NaClO_4$.

□ = 0 M $NaClO_4$

+ = 0.1 M $NaClO_4$

◇ = 0.2 M $NaClO_4$

△ = 0.3 M $NaClO_4$

× = 0.4 M $NaClO_4$

▽ = 0.5 M $NaClO_4$

[γγ-FITC] ≈ 90 nanomolar

Experimental details as per materials and methods.

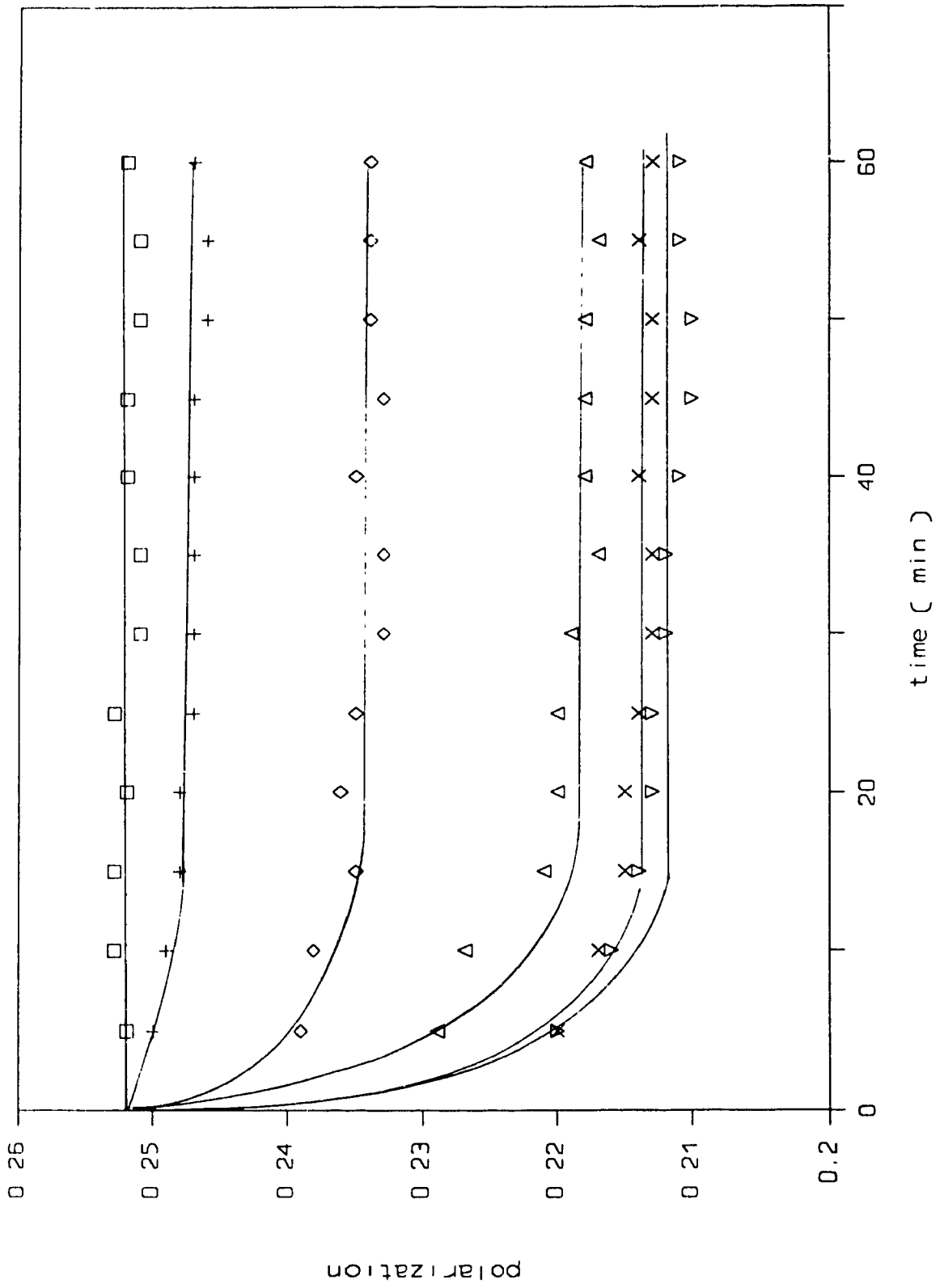
polarization
0.26
0.25
0.24
0.23
0.22
0.21
0.2
0
20
40
60
time (min)

Figure 13: Polarization of γγ-FITC versus $NaClO_4$ and NaCl.

$NaClO_4$ data is a replot of figure 12 at 60 minutes.

□ = $NaClO_4$ (line 1)

+ = NaCl (line 2)

[γγ-FITC] = 90 nM

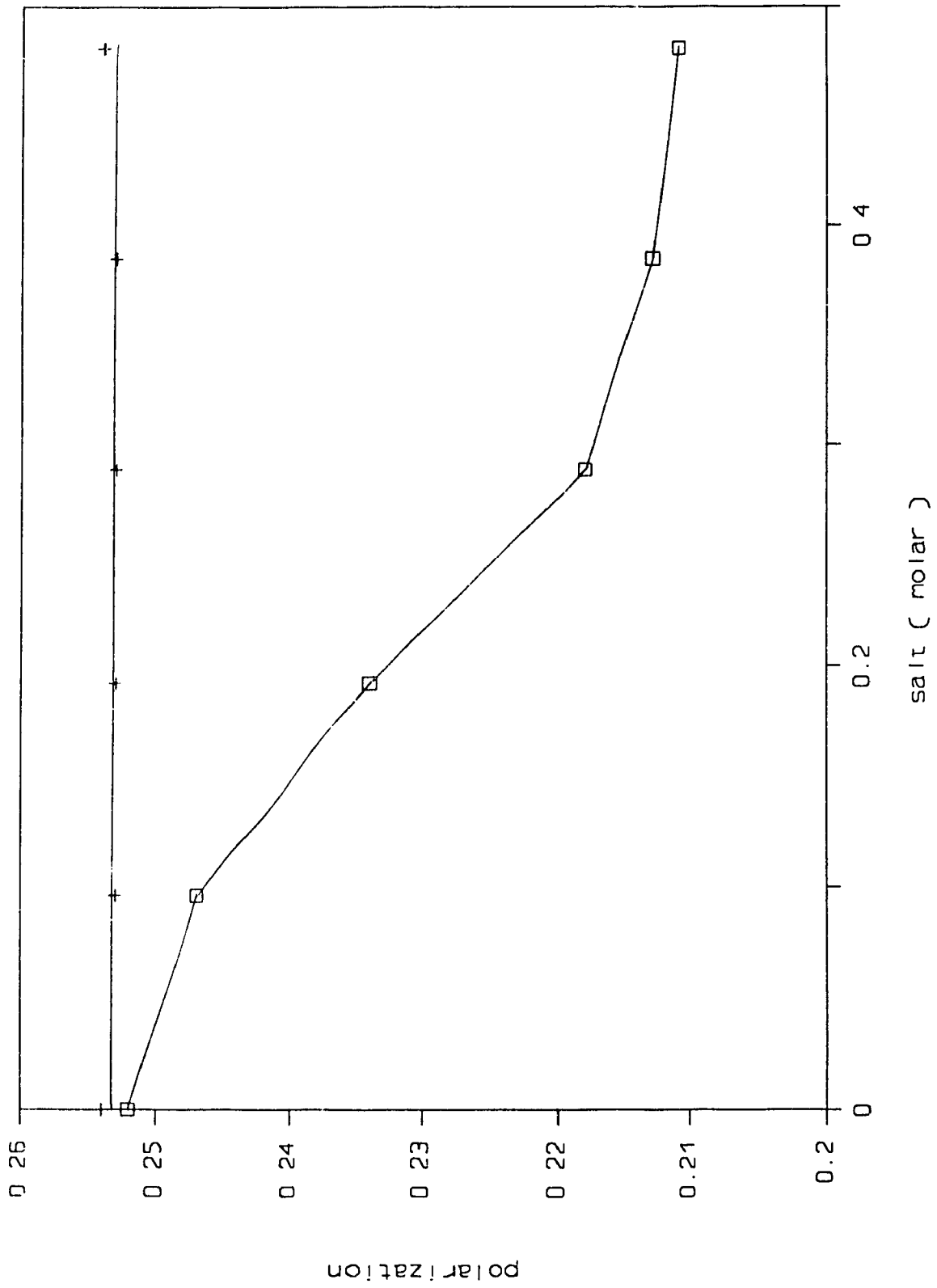
polarization
0.26
0.25
0.24
0.23
0.22
0.21
0.2
0
0.2
0.4
salt (molar)

dissociation is complete by 0.5 M $NaClO_4$. The time required to reach the plateau is also in agreement with the less than 30 minutes required for the loss of the dimer band in the SDS-PAGE crosslinking experiment (fig.10).

Since we do not observe a decrease in polarization in the presence of 0.1 to 0.5 M NaCl (fig.13, line 2) it is also concluded that the causative dissociating agent is the perchlorate anion and that the polarization decrease is independent of any ionic strength effects upon either γγ or FITC.

Since the polarization observed for the monomer (plateau region of fig. 13) is 0.213 ± 0.001 and that of the dimer is 0.252 ± 0.001 the change in polarization upon dissociation, then, is 15.4 ± 0.75%

C.2.2: Estimate of the polarization change expected upon dissociation of γγ-FITC.

As was mentioned at the beginning of this section, a decrease in polarization upon dissociation of γγ-FITC is expected due to a lower T_c for the monomer than the dimer. In section B:1.1 the theoretical value of T_c for the dimer was calculated to be 32.8 nsec. It is to be recalled that the observed value could be as high as 60 nsec., due to the deviation of the macromolecular shape from the assumed spherical structure, but that the T_c could not be lower than 32.8 nsec. Since the monomers of γγ are identical then upon dissociation, according to equation 9, the T_c will simply be 1/2 that of the dimer (i.e. 32.8/2 = 16.4 nsec). This value, of course, assumes a spherical monomer and, as such,

is the lowest possible value. As the shape of the monomer deviates from the spherical the T_c will increase. As for the dimer the expected observed value of T_c for the monomer will likely be closer to 30 nsec.

The numerical values of α and β, as long as they are unchanged upon dissociation (i.e. $\alpha_M = \alpha_M$ and $\beta_M = \beta_D$), do not effect a calculation of the expected change in polarization upon dissociation. This is a simple consequence of the following:

(1) $D = \alpha \ \beta \ Y$ D = Anisotropy of dimer

(2) $M = \alpha \ \beta \ Z$ M = Anisotropy of monomer

Y = rotation of dimer $= (1 + T_f / T_{c(D)})^{-1}$

Z = rotation of monomer $= (1 + T_f / T_{c(M)})^{-1}$

$$\%\text{change} = M/D = \frac{\alpha \ \beta \ Z}{\alpha \ \beta \ Y} = \frac{Z}{Y} \quad \text{:independent of } \alpha \text{ and } \beta$$

Consequently, we can use any values of α and β that we like (i.e. errors in the calculation of α and β can be ignored).

Since $\gamma\gamma$-FITC is completely dissociated in 0.5 M $NaClO_4$ and we have previously established that the T_f of FITC in 0.5 M $NaClO_4$ (fig.9) is unchanged from that in the absence of $NaClO_4$ (fig.4) the following data can be used, along with equations 14 and 15 to calculate the expected polarization change (%) upon dissociation (table 1).

$T_{c\ dimer}$ = 32.8 to 60 nsec. α = 23.14 degrees

$T_{c\ monomer}$ = 16.4 to 30 nsec. β = 24.87 degrees

T_f = 3.9 nsec.

It is to be observed (table 1) that if both the dimer and monomers rotated as hydrated spheres (i.e. T_c = 32.8 and 16.4 nsec, respectively) then the expected polarization change would be 9.1% This, of course, is not a reasonable assumption considering that the observed values of T_c are always greater than the predicted values (B:1.1). A more likely case is if the values of T_c approach 60 and 30 nsec. for the dimer and monomer, respectively. In this case the predicted polarization changes are all less than ≈ 9% It is to be noted that higher % changes are contained in table 1 however, they all suppose that the T_c of the dimer is what would be expected to be observed but that the T_c of the monomer is typical of that of a hydrated sphere. This is considered unlikely. Since we observe an ≈ 15% change in polarization upon dissociation then it is likely that either α or β (or both) is being altered upon dissociation.

In the next section we will attempt to determine whether there is evidence for the above assertion.

Table 1: Table of expected % change in polarization as a function of the T_c values of the dimer and monomer.

$T_{c(M)}$ (nsec.)	32.8	35.0	40.0	45.0	50.0	55.0	60.0
30.0	0.7	1.1	2.5	3.2	3.9	4.5	5.2
26.4	2.2	2.5	3.9	4.6	5.3	5.9	6.6
24.4	3.3	3.6	5.0	5.7	6.3	7.0	7.6
22.4	4.4	4.7	6.1	6.7	7.4	8.0	8.8
20.4	5.4	5.8	7.1	7.8	8.5	9.1	9.6
18.4	7.3	7.6	8.9	9.6	10.2	10.8	11.4
16.4	9.1	9.4	10.7	11.3	12.0	12.6	13.1

$T_{c(D)}$ (nsec.)

D: ACCOUNTING FOR THE OBSERVED POLARIZATION CHANGE UPON DISSOCIATION.

In the last section we used equations 14 and 15 to show that the theoretical decrease in polarization upon dissociation was ≈ 9%. We used the experimental fact that the fluorescent lifetime of FITC on γγ-FITC is equal to its fluorescent lifetime on γ-FITC (figs.4 and 9). Or in other terms:

$$T_{f(M)} = T_{f(D)}$$

and the assumptions that:

$$\alpha_{dimer} = \alpha_{monomer}$$

and/

$$\beta_{dimer} = \beta_{monomer}$$

to arrive at our theoretical value.

In this section we will individually study these assumptions in order to determine which of these possible sources of depolarization is contributing to the observed 15% change in polarization upon dissociation. It will be shown that the rigidity of FITC attachment is decreased in the γ monomer, relative to the dimer, ($\beta_{(M)} > \beta_{(D)}$), so as to account for the observed change in polarization, and that the other assumption is valid.

D.1.0: Investigation into the possible effect of $NaClO_4$ upon α_{dimer}.

A Jablonski diagram (fig.14) tells us that, in theory, the emission spectrum of a fluorophore is independent of the excitational energy used [22]. Both the nonradiative processes of internal conversion and vibrational relaxation occur before photon emission, so that regardless of whether excitation occurs from the ground state (S_0) to the first excited state (S_1) or higher excited states (S_2,S_3 etc.) emission occurs from the lowest vibrational level of S_1 to the various vibrational levels of S_0. The emission band will then be independent of the wavelength of excitation.

Now, when polarized light is used to excite a fluorophore a new scenario arises. If absorption and emission involve the same electronic transition (S_0—— S_1 followed by S_1—— S_0), then emitting and absorbing dipoles are parallel [23]. The orientation of the absorption dipole, relative to the emission dipole, however, differs for each absorption band. Consequently α and therefore polarization varies with the excitational wavelength.

D.1.1: Excitation polarization spectra of γγ-FITC in the absence and presence of 0.5 M $NaClO_4$.

The emission spectra of γγ-FITC in the presence of $NaClO_4$ (fig. 15) is shown to be independent of the excitation wavelength (460-495 nm). The same behaviour is observed in the absence of $NaClO_4$ (spectra not shown since they are identical). This tells us that either excitation from 460 to 495 nm involves

Figure 14: Jablonski diagram for the absorption and emission of a photon.

S_0 = ground state singlet

S_1 = first excited state singlet

S_2 = second excited state singlet

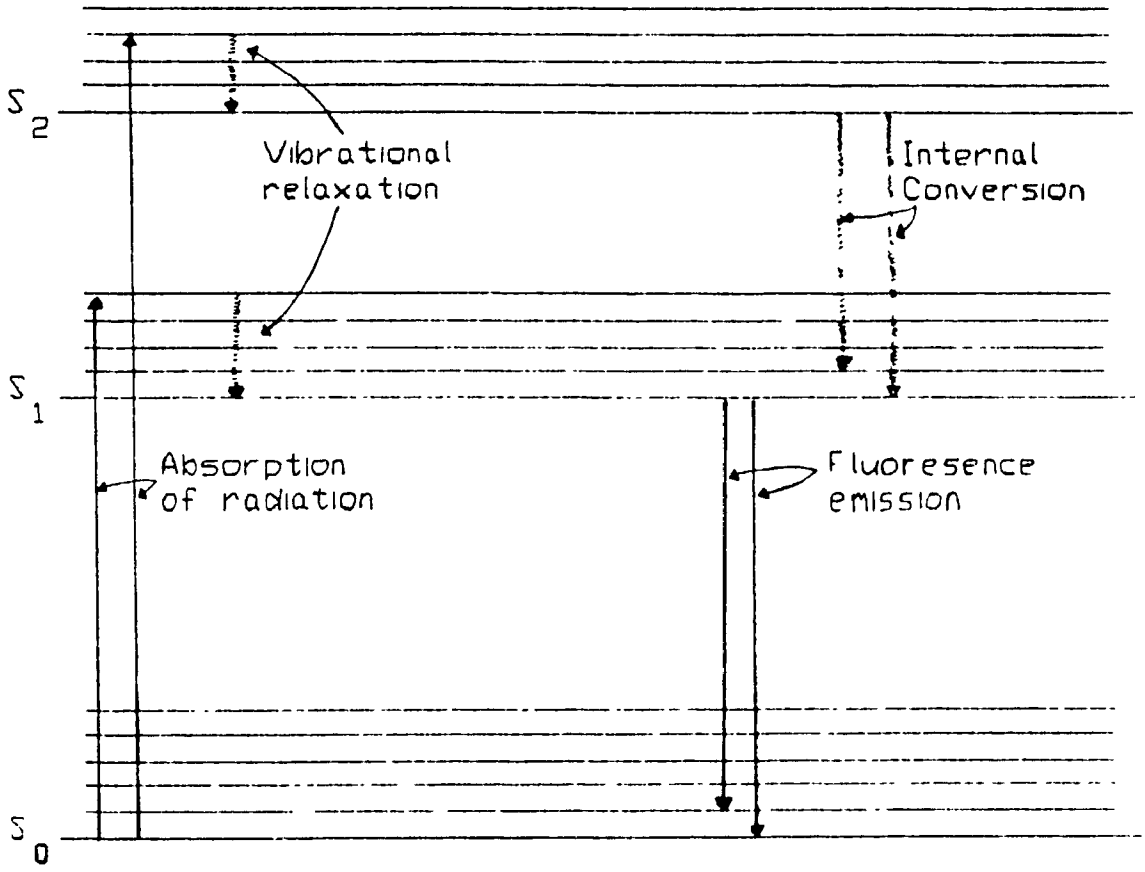
S2
S1
S0
Vibrational relaxation
Internal Conversion
Absorption of radiation
Fluoresence emission

Figure 15: Emission spectra of γγ-FITC as a function of excitation.

Solvent = Buffer A + 0.5 M $NaClO_4$

- - - - - = Excitation spectrum
emission set at 520 nm

——— = Emission spectrum at the specified wavelengths of excitation

[γγ-FITC] = 75 nM

Signal gain = 2

Slits = 8 nm for excitation and emission

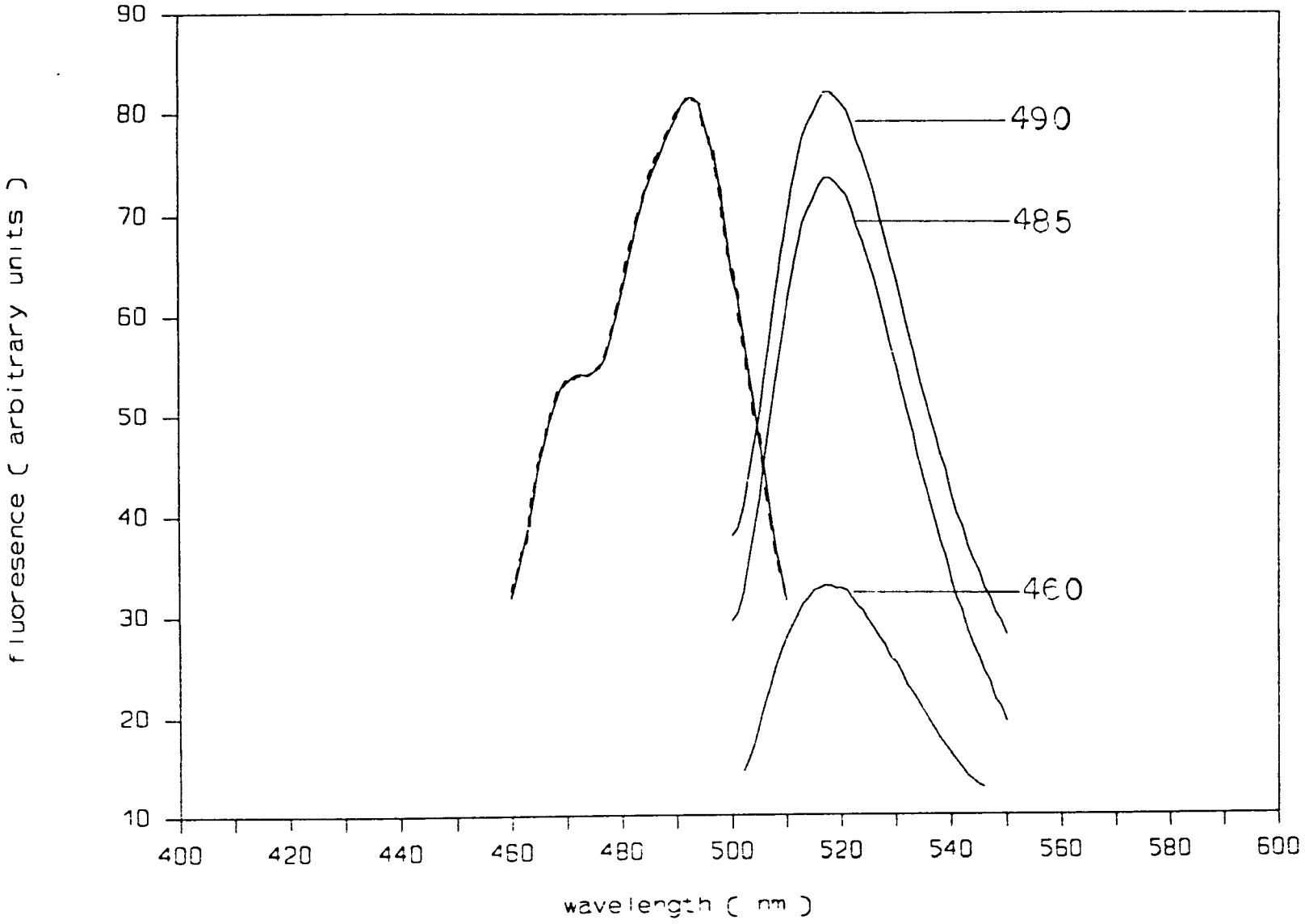
fluoresence (arbitrary units)
90
80
70
60
50
40
30
20
10
400
420
440
460
480
500
520
540
560
580
600
wavelength (nm)
490
485
460

only excitation into the first excited state or that other electronic levels are generated but they all relax back to the lowest excited singlet state prior to emission. What can be stated, however, is that only one emission dipole exists.

The excitation polarization spectrum of γγ-FITC in the absence of $NaClO_4$ (fig.16, line 1) shows us that there are at least 3 overlapping electronic transitions in the 460 to 495 nm excitational range. This has also been shown to be the case with FITC and in other proteins labelled with FITC [34]. Consequently we are indeed getting excitation into other absorption bands. The highest polarization values are observed at the longest wavelengths of excitation. This is to be expected since the longer wavelengths primarily involve excitation into the first absorption band and since emission is from the first excited state the dipoles are likely to be nearly collinear or at least the angle between these dipoles is expected to be less than the angle between the higher excited state absorption dipoles and the emission dipole.

Now here is the problem:

Suppose that the presence of 0.5 M $NaClO_4$ altered the contributions of the various electronic transitions to the emission. In this case then, at any particular wavelength of excitation the particular population of excited state species in 0.5 M $NaClO_4$ may not be the same as in its absence. Consequently we could observe a change in polarization which is independent of dissociation.

The excitation polarization spectrum of γγ-FITC in the presence of 0.5 M $NaClO_4$ (fig.16, line 2) is identical in shape to that in its absence. The only

Figure 16: Excitation polarization spectra of γγ-FITC in the presence and absence of $NaClO_4$.

Emission set at 520 nm

□ = Buffer A ; line 1

+ = Buffer A + NaClO4 (0.5 M) ; line 2

[γγ-FITC] = 75 nM

Signal gain = 3

Slits = 8 nm for excitation and emission.

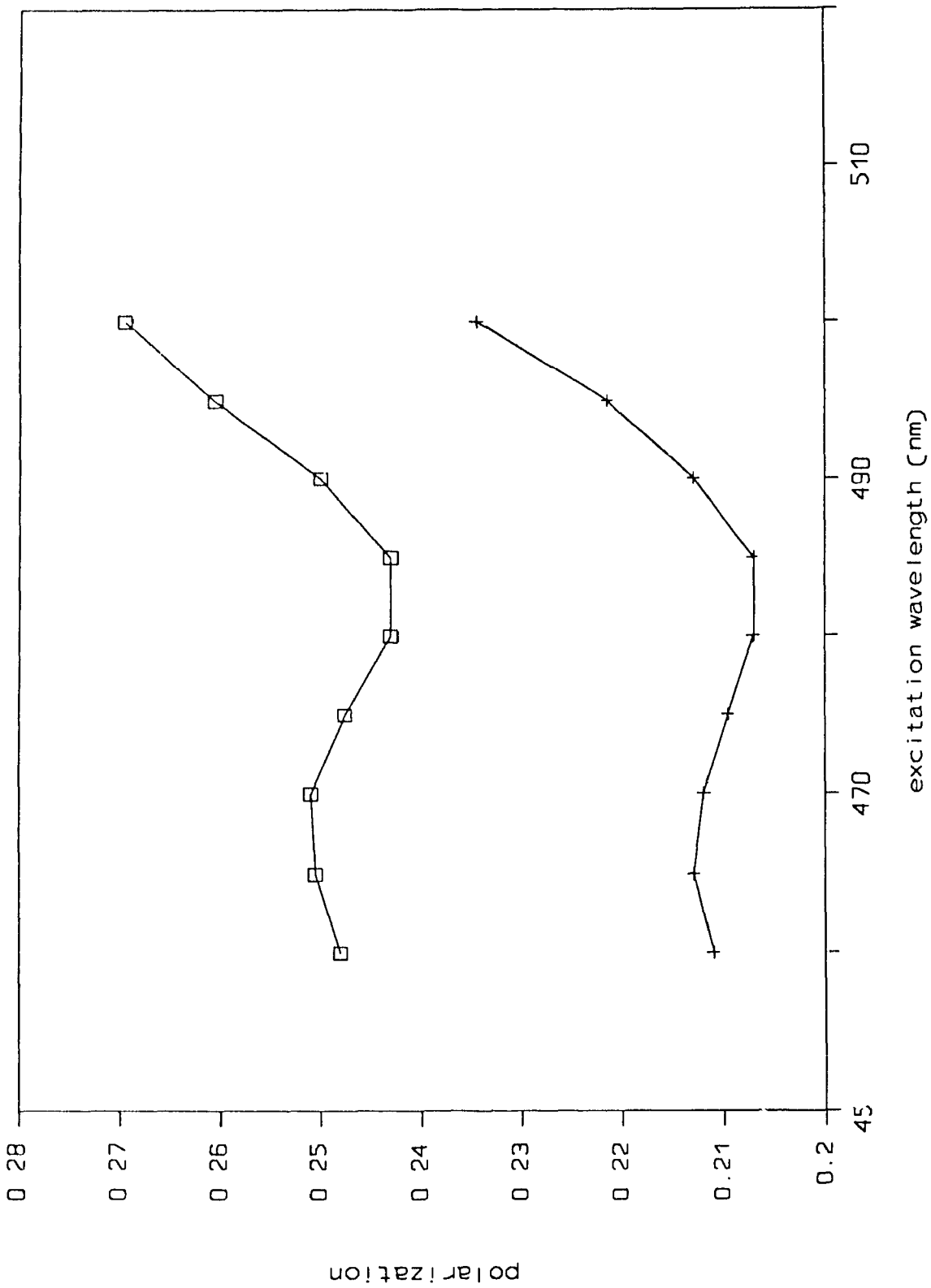
polarization
0.28
0.27
0.26
0.25
0.24
0.23
0.22
0.21
0.2
450
470
490
510
excitation wavelength (nm)

difference being the constantly (15-16%) lower polarization values, resulting from dissociation. It is therefore concluded that the decrease in polarization in 0.5 M $NaClO_4$ (fig.13) does not involve any alteration in α_{dimer} such that;

$$\alpha_{dimer} = \alpha_{monomer}$$

We will next investigate the effect of NaClO4 upon the β term.

D.2.0: Investigation into the possible effect of $NaClO_4$ upon $\beta_{monomer}$.

If upon dissociation the degree of FITC rotation relative to $\gamma\gamma$ (β) is unaltered then, of course, $\beta_D = \beta M$, and consequently, the depolarization observed in $NaClO_4$ (fig.13) is not dependant upon β.

If upon dissociation the local mobility of FITC is increased such that, $\beta_M > \beta D$, then the depolarization observed upon dissociation would be greater than the 9% which was theoretically predicted (C.2.2). In order to determine the degree of FITC mobility relative to the monomer (β_M) we will construct a plot of polarization versus viscosity in the presence of $NaClO_4$.

D.2.1. Calculation of β_M from a plot of polarization versus viscosity in the presence of NaClO4.

We were previously (fig.8) able to determine β_D from a plot of polarization versus viscosity. This same plot can be constructed for the γ-FITC monomer by performing the experiment in the presence of $NaClO_4$.

The P_0' value (fig.17) in the presence of $NaClO_4$, from the 1 / P intercept (3.55 ± 0.003) is found to be 0.2815 ± 0.0025. Conversion to anisotropy, using equation 10 gives;

$$A_0' = 0.207 \pm 0.002$$

Using equation 5 and $A_0 = 0.306 \pm 0.025$ (B:1.3), then;

$$\beta_{monomer} = 27.33 \pm 2.9 \text{ degrees.}$$

It is to be recalled (B:1.3) that β_{dimer} was calculated to be 24.9 ± 3.5 degrees. Since the values of β_M and β_D are not significantly different then one could not propose, based solely on the numbers, that FITC is any more or less flexible in the monomer than it is in the dimer. However, we have shown (D:1.0) that $\alpha_M = \alpha_D$ and, as such, that the value of A_0 is the same for the monomer as it is for the dimer (eq.3). In this case then the increased 1 / P intercept in the presence of $NaClO_4$ (3.55 ± 0.003) relative to its absence (3.34 ± 0.004) can only mean that $\beta_M > \beta_D$ (eq.5).In other words, that the degree of mobility of FITC has indeed increased upon dissociation.

D:2.2: The increase in FITC mobility upon dissociation can account for the observed change in polarization.

It has been established (C:2.2) that as long as the values of α and β are unaltered upon dissociation (i.e. $\alpha_D = \alpha_M$ and $\beta_D = \beta_D$) that their numerical values are unimportant in calculations of the change in polarization expected upon

Figure 17: Polarization of γ-FITC versus viscosity in the presence of 0.5 M $NaClO_4$.

♦ = γ-FITC in 0.5 M $NaClO_4$

□ = γγ-FITC in buffer (replot of figure 8)

Temperature = 298.15 K

Excitation = 492 nm

Emission = 520 nm

$1 / P_0 = 3.55 \pm 0.033$

$P_0 = 0.2815 \pm 0.0025$

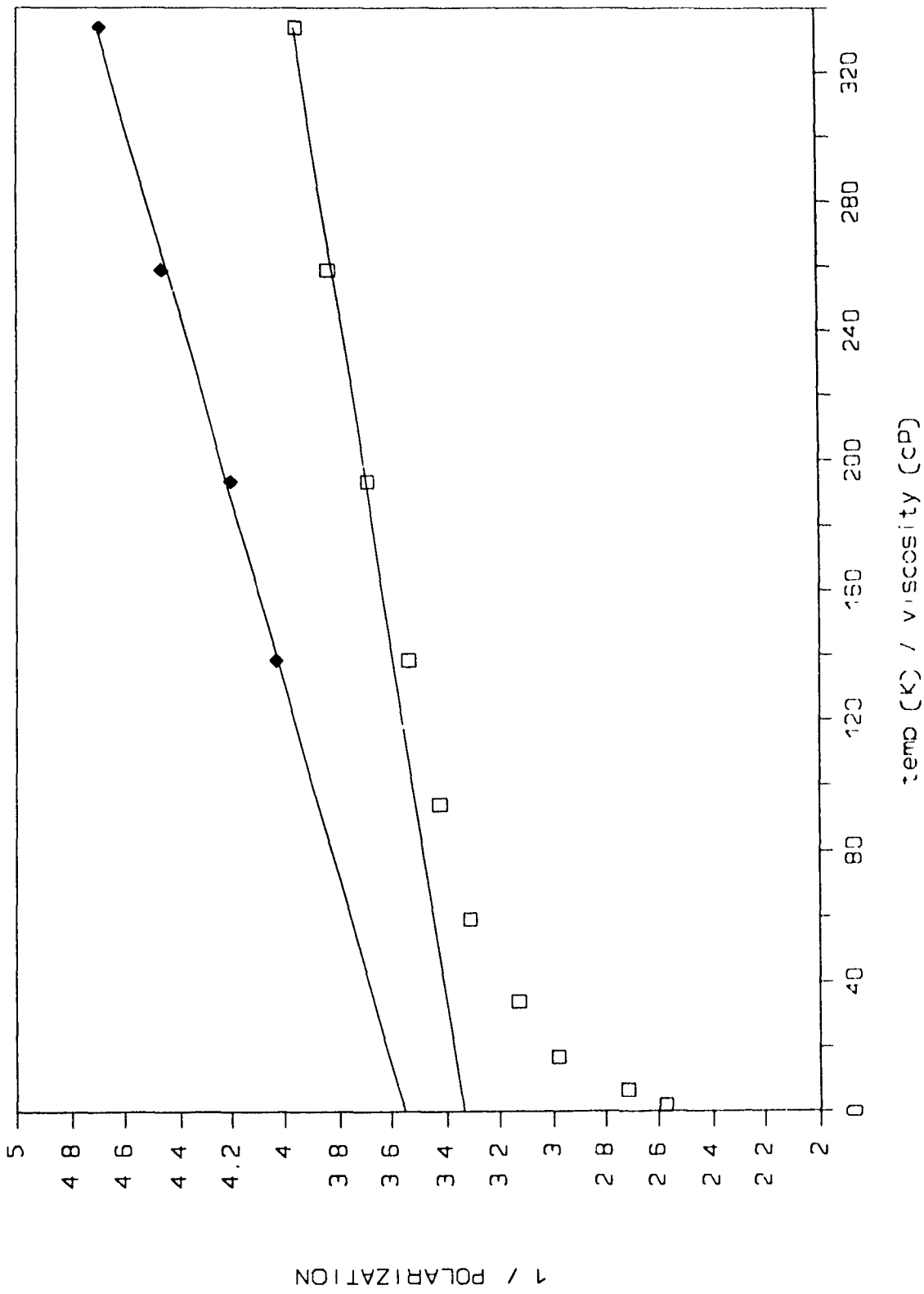
1 / POLARIZATION
Temp (K) / viscosity (cP)
5
4.8
4.6
4.4
4.2
4
3.8
3.6
3.4
3.2
3
2.8
2.6
2.4
2.2
2
0
40
80
120
160
200
240
280
320

dissociation. In the same way, then, a measure of the % change in polarization expected upon dissociation when β_M is not equal to β_D is also independent of the value of α used:

$$D = \alpha \ \beta_D \ Y$$

$$M = \alpha \ \beta_M \ Z$$

$$\% \text{ change} = M/D = \frac{\alpha \ \beta_M \ Z}{\alpha \ \beta_D \ Y} = \frac{\beta_M \ Z}{\beta_D \ Y} \quad \text{:independent of } \alpha$$

Since we can use any value of α then we can use any value of A_0 to calculate β from the observed values of A_0' for the dimer and monomer (eq.5). The values of β, then, are not the true values but this, of course, is of no consequence since it is the ratio β_M / β_D that is pertinent in a calculation of the change in polarization expected upon dissociation.

Using $A_0 = 0.281$ and A_0' (dimer) $= 0.222 \pm 0.003$ gives, using eq. 5;

$$\beta_D = 21.965 \pm 0.585 \text{ degrees}$$

Using $A_0 = 0.281$ and A_0' (monomer) $= 0.207 \pm 0.002$ gives, using eq. 5;

$$\beta_M = 24.77 \pm 0.36 \text{ degrees}$$

These values are used, along with $Tc_{(M)}$ (in the range 16.4 to 30 nsec.) and $T_{c(D)}$ (in the range 32.8 to 60 nsec.) as in table 1, to generate table 2. It is to be observed (table 2) that the predicted changes in polarization upon dissociation can be as high as 18.1 ± 1.8 % (note: all polarization values in table 2 contain

Table 2: Table of expected % change in polarization when $\beta_M > \beta_D$, as a function of the T_c values of the dimer and monomer.

$T_{c(M)}$ (nsec.)	32.8	35.0	40.0	45.0	50.0	55.0	60.0
30.0	6.8	7.5	8.4	9.1	9.9	10.4	10.8
26.4	8.1	8.7	9.7	10.4	11.1	11.6	12.1
24.4	9.1	9.7	10.6	11.3	12.0	12.5	13.0
22.4	10.2	10.8	11.7	12.4	13.0	13.7	14.0
20.4	11.3	11.8	12.7	13.5	14.2	14.7	15.1
18.4	12.6	13.2	14.1	14.8	15.5	16.0	16.4
16.4	14.4	14.9	15.8	16.5	17.2	17.7	18.1

$T_{c(D)}$ (nsec.)

an error of ± 1.8%) but as in table 1, high values of $T_{c(D)}$ although probable are not likely to be coupled with low values of $T_{c(M)}$. The most likely values are contained within the shaded area. Considering that the observed change in polarization upon dissociation is 15.4 ± 0.75 (C.2.1) it is concluded that the increased flexibility of FITC upon dissociation can account for this change.

D.3.0: The increase in β is very likely intrinsic to dissociation.

In section C we saw that the dissociation of γγ was complete by 0.5 M $NaClO_4$. It has, however, been undefined as to whether the structure of the monomer is or is not effected by dissociation.

We have just seen that upon dissociation β is increased (D.2.2). In theory, for a fluorophore bonded to a macromolecule the rotational motion of this fluorophore decreases, relative to the free fluorophore in solution, due to it's covalent attachment as well as to the local geometry of the macromolecule at the site of binding (noncovalent). Upon dissociation, then, if a fluorophore bonded monomer does not undergo any structural alterations then the local geometry at the fluorophore binding site must also be unchanged and as such β will not be altered upon dissociation (it is to be noted that the opposite is not necessarily true). Since β is altered upon dissociation, we can then infer that a structural alteration of the γ monomer has occurred upon dissociation in 0.5 M $NaClO_4$. An exception, however, exists; if the FITC probe is attached near the subunit interface then upon dissociation the local geometry around FITC may be

altered without any modification of the tertiary structure of the monomer.

The question, then, is whether the increased flexibility of FITC is intrinsic to the process of dissociation or due to possible denaturation effects in the presence of NaClO4. This is an important question since if the increased flexibility of FITC is a result of denaturation then we should not expect to observe this denaturation in the absence of $NaClO_4$. Consequently, we would observe a less than 15% change in polarization upon dissociation induced by pressure or other agents.

One might suggest, at this point, that if the increased flexibility of FITC is intrinsic to dissociation then we would predict that the monomer produced by $NaClO_4$ is catalytically active since there is no evidence that the active site is at the subunit interface or that the enzyme exhibits any form of co-operativity. This activity is shown (fig.18) to be negligible. This finding, however, is difficult to interpret due to the effect of the sodium ion, itself, upon the activity of $\gamma\gamma$ (fig.18).

It was shown earlier (fig.13) that NaCl (0.5 M) does not result in any alteration of the polarization of $\gamma\gamma$-FITC and, as such, does not dissociate $\gamma\gamma$-FITC. However, Na^+, as well as Li+ and other monovalent cations, act as inhibitory ions by specific binding to the mammalian enolases [6]. Consequently, the γ monomer, uneffected by denaturation, would still have any intrinsic activity masked due to the presence of Na^+.

Figure 18: Activity of γγ-FITC in the presence or absence of $NaClO_4$ or NaCl.

[γγ-FITC] = 15 nM

+ = NaCl

□ = $NaClO_4$

Activity measurement and experimental protocol as per materials and methods.

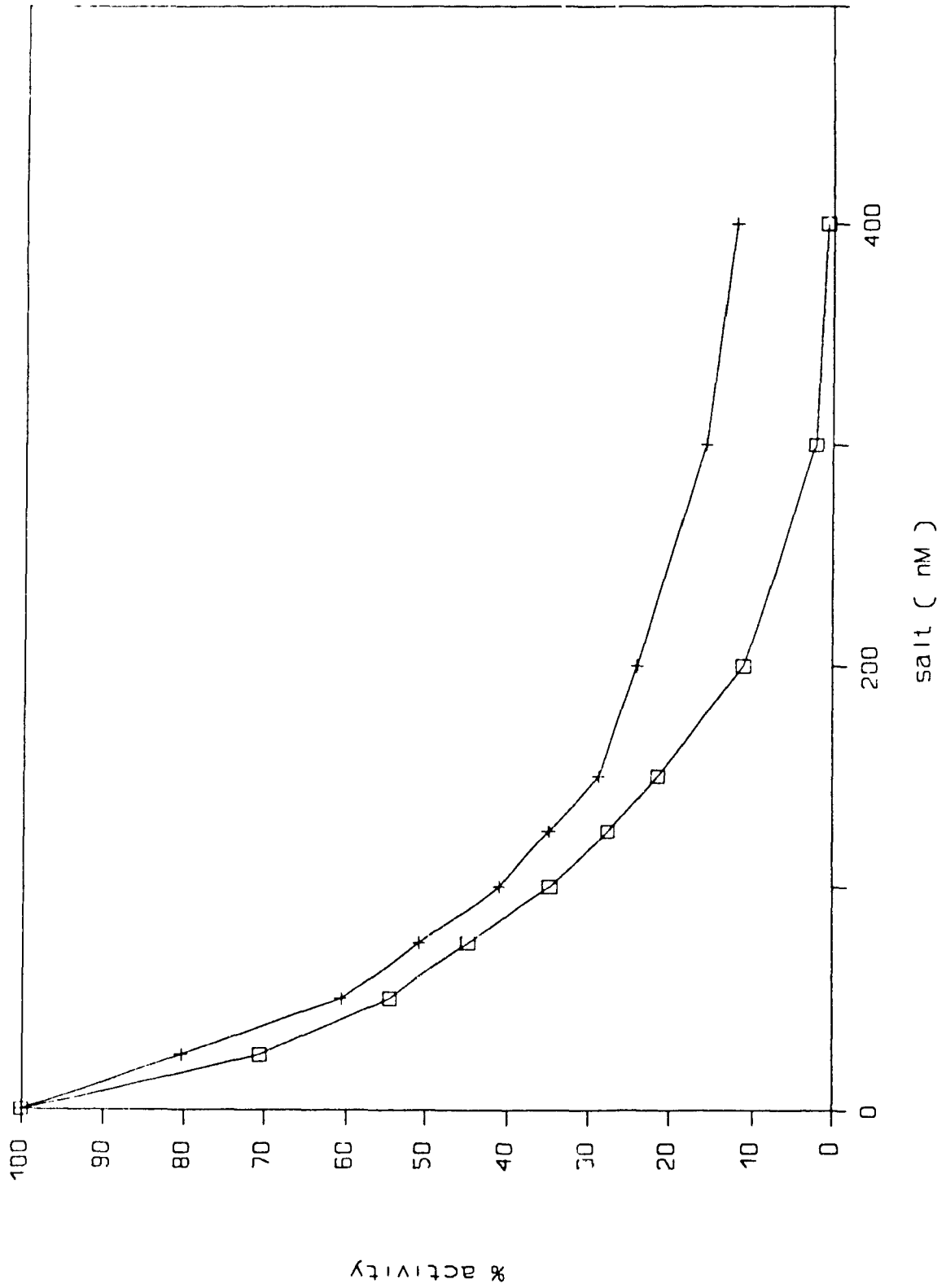
% activity
100
90
80
70
60
50
40
30
20
10
0
0
200
400
salt (mM)

Upon removal of the $NaClO_4$, via dialysis against buffer A, the activity is 85-90% regained and the polarization characteristic of the dimer is fully recovered.

The emission lambda maximum for tryptophan in water is 350 nm [35]. Figure 19 shows that the lambda maximum for γγ in buffer is ≈ 335 nm. The higher energy emission lambda maximum results from an incomplete exposure of all 6-8 tryptophans [36] in γγ. The quaternary structure is such that the average tryptophan environment (i.e. collective of all tryptophans) is less polar than complete exposure to the buffer.

The increased emission lambda maximum for tryptophan in water, relative to γγ, stems from increased solvent relaxation effects on the excited state tryptophan in polar media relative to nonpolar, which in turn depends on the dielectric constant of the solvent [37].

In 8 M urea the emission lambda maximum of γγ is red shifted to ≈ 350 nm and a decreased intensity is observed (fig 19). This is consistent with an unfolded protein structure [35]. The average tryptophan environment is now more polar (exposed to solvent) than the native state and consequently solvent relaxation processes decrease the energy of the excited state to a lower energy level (before emission occurs) than in the native state. The decreased intensity is expected due to the decreased lifetime of tryptophan upon solvent exposure [35]. The broadening of the half-width of the emission spectrum is also expected due to the increased contribution of tyrosine residues to the emission spectrum [35].

Figure 19: Tryptophan emission spectra of γγ in buffer, $NaClO_4$, NaCl and urea.

[γγ] = 75 nM

—— = Emission in buffer A, pH 7.15

Emission in buffer A + 0.5 M Nacl, pH 7.15

—— = Emission in buffer A + 0.5 M $NaClO_4$, pH 7.15

---- = Emission in buffer A + 8 M urea

Excitation = 285 nm

Slits = 10 nm

All emission spectra corrected for raman peak and any fluorescence of the buffer system, in the emission range studied.

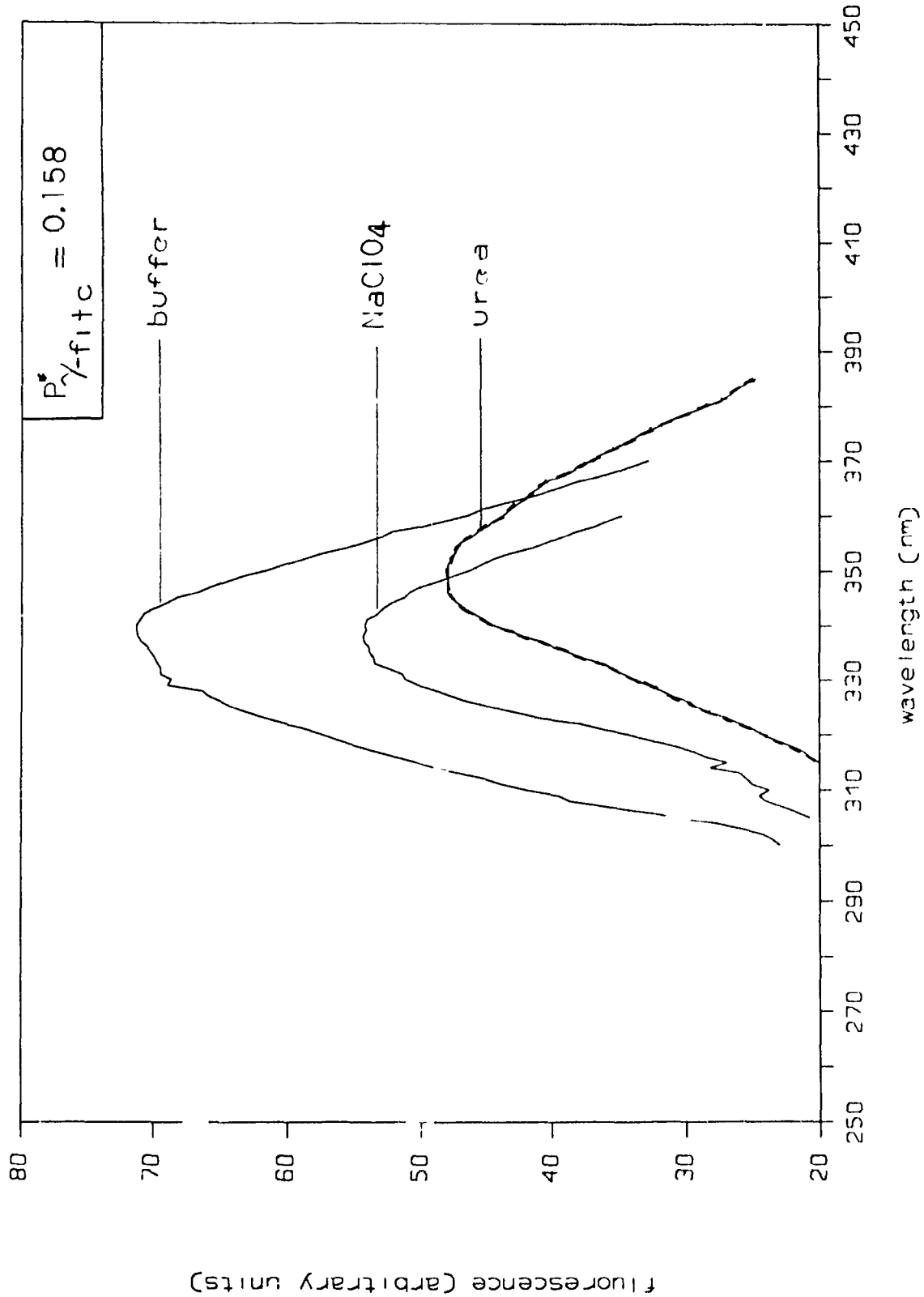
$P^{\circ}_{\gamma\text{-fitc}} = 0.158$
buffer
NaClO4
urea
fluorescence (arbitrary units)
wavelength (nm)
80
70
60
50
40
30
20
250
270
290
310
330
350
370
390
410
430
450

Also shown in figure 19 is the emission spectrum of γγ in 0.5 M $NaClO_4$. We observe a slight red shift (1-2 nm) and a decreased intensity, relative to buffer. 0.5 M NaCl (fig.19) is shown to be without effect upon the tryptophan emission of γγ and, as such, eliminates any contribution due to the Na^+ alone. The emission spectrum of tryptophan alone is unchanged by the presence of 0.5 M $NaClO_4$ (data not shown). We can then conclude that the red shift and decrease in intensity of the tryptophan emission spectrum of γγ, in the presence of 0.5 M salt, is a result of dissociation or, alternatively, some degree of denaturation.

Paladini and Weber, [12] working with yeast enolase, has shown that at 1 M KCl, where the enzyme is known to be dissociated, there is a slight red shift and a decrease in intensity of the tryptophan emission. As well, at a pressure of 2 Kilobar, where the enzyme is also dissociated, there is, again a slight red shift and a decrease in intensity of the tryptophan emission exactly matching that in the salt. In the case of yeast enolase, then, the fluorescent changes were concluded to be intrinsic to dissociation.

There are 6 complete sequences of enolase determined. On average there is a 60% sequence identity between yeast enolase and the vertebrate enolase isozymes. In particular the sequence homology between yeast enolase and γγ is 62% [38]. Brewer [39] has suggested that the decreased intensity and red shift upon dissociation of yeast enolase are due to the exposure of trp-367, which from the very recent crystal structure of yeast enolase at 2.25-A° resolution [38]

lies at the subunit interface. The primary sequence of γγ enolase shows a tryptophan residue at the equivalent position of trp-367 in yeast enolase [36]. One might, therefore, predict that the dissociation of γγ would also result in a red shift and decrease in the intensity of the tryptophan emission. The increased flexibility of FITC and the red shift and decreased intensity of the tryptophan emission upon dissociation can then likely be explained, without invoking any degree of denaturation, as being a result of:

(1) An unaltered tertiary structure of the monomer with the increased flexibility of FITC being due to a relief of rotational constraints previously imposed by its binding near the subunit interface, and the red shift and decreased intensity of the tryptophan emission a result of the exposure of the subunit interface tryptophan to the solvent.

or/

(2) A structural alteration of the monomer with the increased flexibility of FITC being due to a changed geometry at its site of binding (either at the subunit interface or elsewhere on the protein), and the red shift and decreased intensity of the tryptophan emission a result of the exposure of tryptophan residue(s) anywhere in the protein. This includes the subunit interface, alone; the subunit interface along with other areas of the protein; and other areas, alone.

The inset of figure 19 tells us that in 8 M urea the polarization of denatured enolase (γ-FITC*) is 0.157, which is a full 40% difference between

the active γγ-FITC.

In summation, then, we should expect to observe pressure dissociation of γγ-FITC to γ-FITC via a concomitant 15% change in polarization upon complete dissociation, barring pressure effects other than dissociation, and further polarization changes upon pressure induced denaturation to generate γ-FITC*.

SUMMARY:

We set out to develop a fluorescence polarization probe for γγ enolase that could be used under pressure (or other conditions) to directly relay information regarding its quaternary state.

The existence of a monolabelled fluorescein isothiocyanate species of mammalian enolase (γγ-FITC) has been established via its absorption and emission spectra characteristic of FITC and its much increased polarization (0.253) relative to that of FITC alone (0.023). The increase in polarization of FITC bonded to γγ results from the now restricted rotational capability of FITC during it's fluorescent lifetime.

The γγ-FITC species was also shown by gel filtration and activity measurements to remain in the active dimeric state (i.e. the process of labelling does not alter the native structure of γγ).

In terms of polarization (anisotropy), dissociation was seen as the following;

$$A_{dimer} = 2/5 \left(\frac{3\cos^2\alpha_{(D)}-1}{2} \right) \left(1 + \frac{T_{f(D)}}{T_{c(D)}} \right) \left(\frac{3\cos^2\beta_{(D)}-1}{2} \right) \quad \text{(eq.15)}$$

DISSOCIATION

$$A_{monomer} = 2/5 \left(\frac{3\cos^2\alpha_{(M)}-1}{2} \right) \left(1 + \frac{T_{f(M)}}{T_{c(M)}} \right) \left(\frac{3\cos^2\beta_{(M)}-1}{2} \right) \quad \text{(eq.16)}$$

The observed polarization of γγ-FITC (0.253 ± 0.001) was much lower than that which was theoretically predicted (0.465 ± 0.01) for a macromolecule of the molecular weight of γγ. This lower polarization was shown to be a result of:

(a) An intrinsic angle (α = 23.4 ± 3.3 degrees), at the excitational wavelength used, between at least 3 overlapping excitational dipoles and the emission dipole such that the excitational light undergoes a degree of depolarization independent of the rotational motion of γγ and the lifetime of FITC (P_0 is not equal to the theoretical value of 0.5).

and/

(b) The nonrigid attachment of FITC to γγ such that FITC is capable of rotation independent of γγ (β = 24.87 ± 3.5 degrees). During its fluorescent lifetime, then, FITC rotates through a greater angle than if it were rigidly attached to γγ

and consequently depolarizes the light beyond the capacity of the macromolecular rotation.

In the presence of 0.5 M $NaClO_4$, gel filtration and SDS-PAGE crosslinking have shown that γγ-FITC undergoes complete dissociation. The polarization concomitantly decreases over the 0 - 0.5 M $NaClO_4$ concentration range and plateaus at about 0.4 - 0.5 M, for a resultant 15 % change in polarization.

Upon dissociation we theoretically expected no more than a 9 % change in polarization (assuming $\alpha_M = \alpha_D$ and $\beta_M = \beta_D$). The observed 15 % change was shown to be a result of an increase in the flexibility of FITC upon dissociation (leading to further depolarization during the lifetime of FITC) and that this was likely an intrinsic part of the dissociation process.

No alterations of α or the fluorescent lifetime of FITC were observed upon the dissociation in $NaClO_4$.

It is concluded, then, that since $NaClO_4$ dissociates γγ-FITC and is without any other measurable effect, that pressure induced dissociation (in the absence of $NaClO_4$), barring any pressure effects other than dissociation, would result in this same 15 % change in polarization. Theoretically we should then be able to follow the dissociation of γγ to completion. As well, since the denaturation of γγ-FITC (8 M urea) results in an expected decrease in the polarization well beyond that of the monomer, then the polarization of γγ-FITC is also sensitive to denaturation. We should, consequently, also expect to observe

pressure induced structural alterations in addition to those of dissociation.

REFERENCES:

1) WOLD, F. (1971) Enolase. **In** The Enzymes. Vol.5. 3rd ed. Edited by P.D. BOYER. Academic Press, New York. pp. 499-538.

2) SUZUKI, F., UMEDO, Y., and KATO, K. (1980) J. Biochem. (Toyko), **87:** 1587.

3) KELLER, A., SCARNA, H., MERMET, A., AND PUJOL, J.F. (1981) J. Neurochem. **36**: 1389.

4) FLETCHER, L., RIDER, C.C., and TAYLOR, C.B. (1976) Biochim. Biophys. Acta, **452**: 245.

5) RIDER, C.C. and TAYLOR, C.B. (1974) Biochim, Biophys. Acta, **365**: 285.

6) KORNBLATT, M.J., and KLUGERMAN, A. (1989) Biochem. Cell Biol. **67**: 103.

7) BORSCHIK, I.B., PESTOVA, T.V., and SKLYANKINA, V.A. (1985) FEBS Letters, **184** (1): 65.

8) PORTER, D.H., and CARDENAS, J.M. (1981) Biochemistry, **16**: 2532.

9) GRAWRONSKI, T.H., and WESTHEAD, E.W. (1969) Biochemistry, **8:** 4261.

10) NAGY, S.K., and ORMAN.R. (1971) Biochemistry, **10** (13): 2506.

11) MARANGOS, P.J., and PARMA, A.M., and GOODWIN, F.K. (1978) Journal of Neurochemistry, **31**: 727.

12) PALADINI, A.A., and WEBER, G. (1981) Biochemistry, **20**: 2587.

13) KORNBLATT, J., KORNBLATT, J., and HUI BON HOA, G. (1982) Eur. J. Biochem. **128**: 577.

14) KORNBLATT, M.J., and HUI BON HOA, G. (1987) Archives of Biochemistry and Biophysics, **252** (1): 277.

15) MIRER, C.S., and DALTON N.N. (1953) Glycerol, Reinhold, N.Y. pp. 279-281.

16) COOPER, G.T. (1979) Electrophoresis. **In** The Tools of Biochemistry, John Wiley and Sons, Inc. pp. 194-233.

17) LAKOWICZ, J.R. (1983) Principles of Fluorescence Spectroscopy, Plenum Press, New York. pp 15-16.

18) SHORE, J.D., and CHAKRABARTI, S.K. (1976) Biochemistry, **15** (4): 875.

19) McEVILY, A.J., HARRISON, J.H. (1986) The Journal of Biological Chemistry, **261** (6): 2593.

20) Molecular Probes Catalogue. pp. 21.

21) McAIEESE, S.A., DUNBAR, B., FOTHERGILL, J.E., HINKS, L.J., DAY, I.N.M. (1988) Eur. J. Biochem. **178**: 413.

22) Biophysical Chemistry. pp. 458.

23) Ibid 17, pp. 111-150.

24) RAINER, J., and RAINER, R. (1986) Refolding and association of oligomeric proteins, **In** Methods of Enzymology, **131**: 218.

25) PAULY, H.E., and PFLEIDERER, G. (1977) Biochemistry, **16**: 4599.

26) BARTHOLMES, P., and JAENICKE, R. (1978) Eur. J. Biochem. **87**:563.

27) JAENICKE, J. (1967) Polymer Sci. Part C, **16**: 2143.

28) KAMOUN, P.P., (1988) TIBS, **13**: 424.29) HATEFI, Y., and HANSTEI. W.G., (1969) Biochemistry, **62**:1129.

30) HERSKOVITS, T.T., CARBERRY, S.E., and SAN GEORGE, R.C. (1983) Biochemistry, **22**: 4107.

31) SCHACHMAN, H.K., and BURNS, D.L. (1982) The Journal of Biological Chemistry, **257** (15):8638.

32) NANDI, P.K., and PRAKASH, V. (1977) The Journal of Biological Chemistry, **252** (1): 240.

33) HARRINGTON, J.P. (1981) Biochimica et Biophysics Acta, **671**: 85.

34) LAMBOOY, P.K., STEINER, R.F., and STERNBERG, H. (1982) Archives of Biochemistry and Biophysics, 517.

35) Ibid 17, pp. 257-295.

36) SAKIMURA, K., KUSHIYA, E., and TAKAHASHI, Y. (1985) Nucleic Acids Research, **13** (12): 4365.

37) Ibid 17, pp. 187-214.

38) LEBIODA, L., STEC, B., and BREWER, J. (1989) The Journal of Biological Chemistry, **264** (7): 3685.

39) BREWER, J.M., BASTIAENS, P., and LEE, J. (1987) Biochemical and Biophysical Research Communications, **147** (1): 329.

APPENDIX

1.0 : Instrumental measurement of anisotropy or polarization.

The measurement of fluorescence polarization or anisotropy illustrated diagrammatically in figure 1.

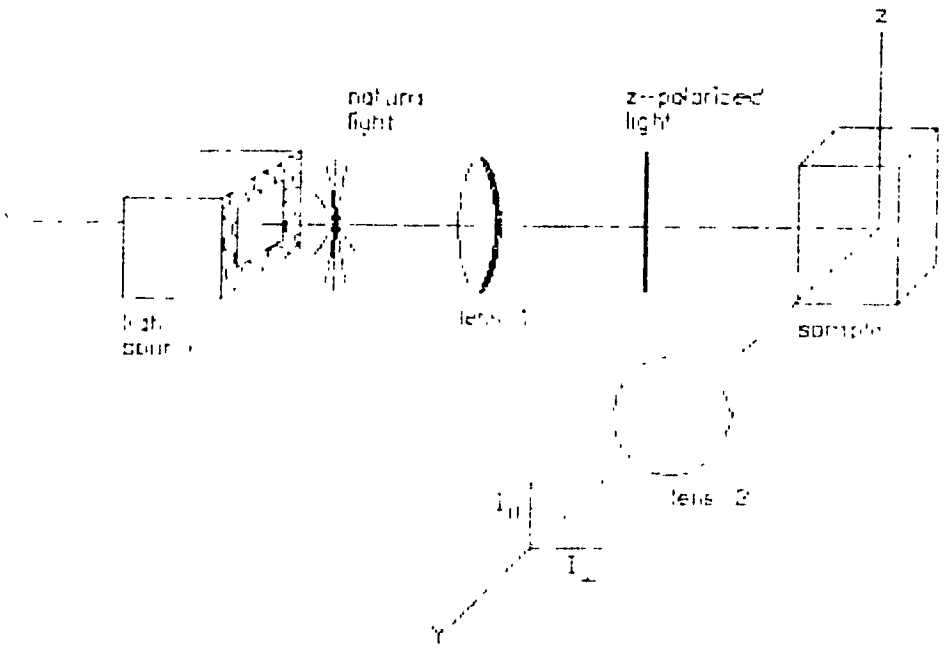

Figure 1: Setup for the measurement of the polarization or anisotropy of a fluorescent sample.

The sample is excited with light that has been vertically polarized via the use of a polarizing lens (lens 1) with its polarizing axis (1.1) orientated parallel to the z axis. The electric vector of the excitational light is, consequently, oriented parallel to the z axis.

One then measures the intensity of the emission through a second polarizing lens (lens 2). When this polarizer has its polarizing axis oriented parallel (||) to the direction of the polarized excitation the observed intensity is $I_{||}$. Likewise, when the observing polarizer has its polarizing axis oriented perpendicular ($\perp$) to the excitation, the intensity is designated $I_{\perp}$.

The anisotropy (A) is calculated according to:

$$A = \frac{I_{||} - I_{\perp}}{I_{||} + 2\, I_{\perp}} \qquad \text{(eq.1)}$$

1.1: How the lenses work.

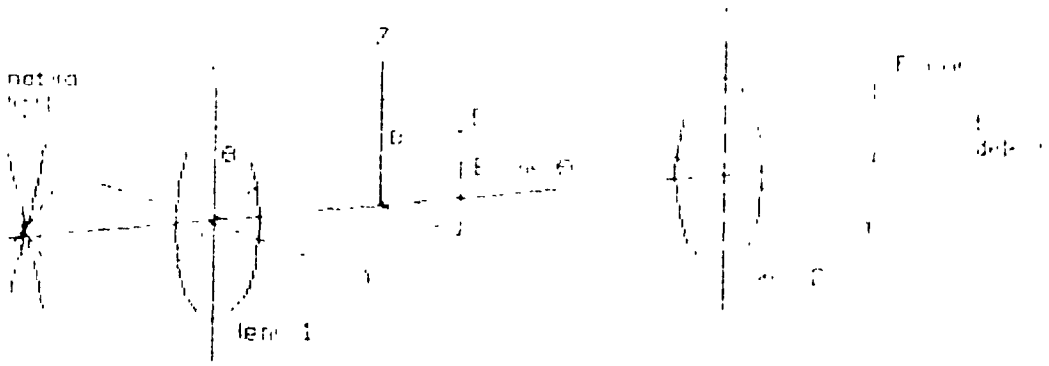

Figure 2: Functioning of the lenses.

In figure 2, the natural (unpolarized) light is incident on the polarizer (lens 1) whose axis is represented by the broken line. The polarized light transmitted may be resolved into two components; one parallel and one

perpendicular to the polarizing axis. Polarizers only transmit the components of the incident waves in which the electric vector (E-vector) is parallel to the polarizing axis. In this case then, the second polarizer (lens 2) will transmit only the electric vector component parallel to the z axis. This means E cos θ and not E.(θ = angle between E and the polarizing axis which in this case is the z axis). For the above situation, then, the transmitted intensity is maximum when $\theta = 0$ and falls to 0 when $\theta = 90$ degrees (i.e. no z component).

It is to be noted, that if we remove the second polarizer, in figure 2, the intensity of light monitored by the detector, upon any rotation of the first polarizer is unchanged. This is so because, as mentioned, the polarizer transmits the components of the incident waves in which the E vector is parallel to the polarizing axis and since by symmetry the components are equal for all azimuths, consequently the intensity does not change.

It should also be noted that the unpolarized incident light passing through the first polarizer has its intensity halved. This is due to the fact that the incident light can always be resolved into components polarized parallel and perpendicular to the polarizing axis. Since the incident light is a random mixture of all states of polarization, these two components are, on average, equal and therefore exactly half of the incident intensity, that, corresponding to the component parallel to the polarizing axis, is transmitted.

1.2: Definitions of polarization and anisotropy.

Consider partially z-polarized light travelling along the x axis (fig.3).

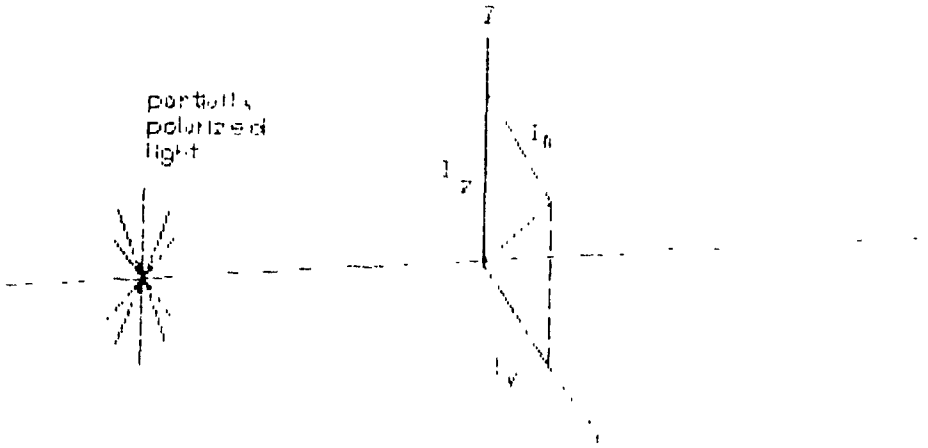

Figure 3: Coordinate system used to define polarization.

The polarization (P) of this light is defined as the fraction of the otal light which is linearly polarized or mathematically stated:

$$P = \frac{I_P}{I_P + I_N} \qquad \text{(eq.2)}$$

Where: I_P = Intensity of polarized component

I_N = Intensity of the natural light

In order to determine the polarization, then, one must measure the intensities along both the z axis (I_Z) and the y axis (I_Y).

I_Z = Intensity from the z-polarized light plus the z components cf the natural light.

I_Y = Intensity of the natural unpolarized light components on the y axis only (the z-polarized light has no components on the y axis)

Since we know that for unpolarized light only 1/2 the unpolarized intensity is transmitted by the polarizer (1.1), we can then state:

$$I_Y = 1/2\ I_N \qquad \text{(eq.3)}$$

$$I_Z = I_P + 1/2\ I_N \qquad \text{(eq.4)}$$

Rearranging equations 3 and 4 in terms of I_P and I_N we have:

$$I_N = 2I_Y \quad (\text{or } 1/2\ I_N = I_Y) \qquad \text{(eq.5)}$$

$$I_P = I_Z - 1/2\ I_N \quad (\text{or } I_P = I_Z - I_Y) \qquad \text{(eq.6)}$$

Substituting equations 5 and 6 into equation 2 gives:

$$P = \frac{I_Z - I_Y}{I_Z + I_Y} \qquad \text{(eq.7)}$$

For vertically polarized (z-polarized) excitation:

$$I_Z = I_{\parallel} \qquad \text{(eq.8)}$$

$$I_Y = I_{\perp} \qquad \text{(eq.9)}$$

Substituting equations 8 and 9 into equation 7 gives:

$$P = \frac{I_{||} - I_{\perp}}{I_{||} + I_{\perp}} \qquad \text{(eq.10)}$$

The anisotropy (A) of a light source is defined as the ratio of the polarized component to the total intensity (I_T).

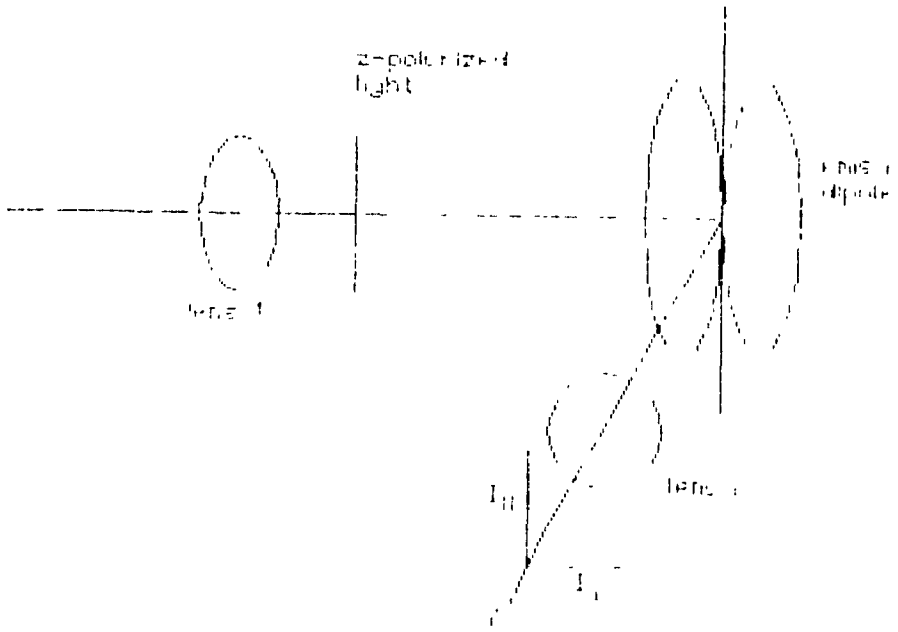

Figure 4: Coordinate system used to define anisotropy.

Figure 4 shows us that the radiation emitted by a fluorophore is symmetrically distributed about the z axis. In other words, the light emitted by a dipole is equally distributed along the x and y axis. Therefore:

$$A = \frac{I_Z - I_Y}{I_Z + I_Y + I_X} = \frac{I_Z - I_Y}{I_T} \qquad \text{(eq.11)}$$

and/

$$I_Y = I_X \qquad \text{(eq.12)}$$

Consequently:

$$A = \frac{I_Z - I_Y}{I_Z + 2I_Y} = \frac{I_{\parallel} - I_{\perp}}{I_{\parallel} - 2I_{\perp}} \qquad \text{(eq.13)}$$

Polarization can also be defined as the ratio of the polarized component to the total intensity, the only difference being that the theory of polarization describes a light source when the light is directed along a particular axis and therefore the total intensity is given by $I_Z + I_Y$ and not that in equation 11.

Polarization and anisotropy can be interchanged using the following relationships:

$$P = \frac{3A}{2 + A} \qquad \text{(eq.13)}$$

and/

$$A = \frac{2P}{3 - P} \qquad \text{(eq.14)}$$

At this point in the theory, then, we can state that;

(1) For completely polarized light; $I_{\perp} = 0$ (figure 3 and equations 10 and 13) and consequently; $P = A = 1$

(2) For unpolarized light; $I_{\perp} = I_{\parallel}$ and $P = A = 0$ For intermediate values, however, P is not equal to A.

We will next look at a more chemical/biochemical relevant use of anisotropy.

2.0 : Theory of anisotropy of fluorophores in solution.

In this section we will develop the theory of anisotropy as it applies to a fluorophore solution. Mathematically, anisotropy, rather than polarization is easier to deal with and as such it will generally be stressed.

The theory begins with the following vector diagram:

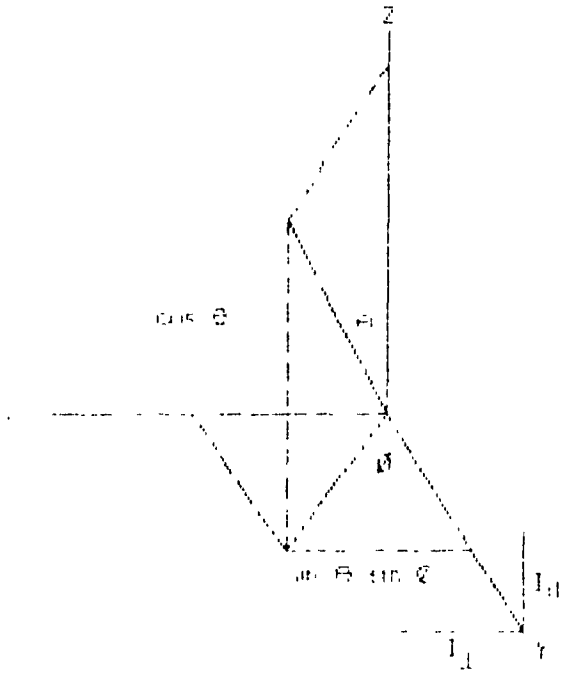

Figure 5: Coordinate system used in the derivation of equations of anisotropy and polarization.

The vector represents a collinear absorbtion-emission dipole in a vitrified solution, such that the fluorophore is incapable of undergoing any rotation during its fluorescent lifetime (T_f).

The theory will be developed in the following fashion:

(1) We will firstly consider a fluorophore with collinear dipoles in a vitrified solution (fig.5) and develop an equation of anisotropy to describe the situation.

(2) Secondly, we will determine how the equation is modified when we have non linear dipoles.

(3) Lastly, we will throw in the possibility of mobility of the fluorophore, during its fluorescent lifetime, either on its own or attached to a macromolecule. We will ultimately end up with an expression that will describe the observed anisotropy of any fluorophore in solution.

2.1: Fluorophore with collinear dipoles in a vitrified solution.

Since the intensity of light radiated from a dipole is proportional to the square of its vector projected onto the axis of observation [23], we can make the following statements with reference to figure 5.

$$I = \cos^2 \theta \qquad \text{(eq.15)}$$

$$I = \sin^2 \theta \sin^2 \qquad \text{(eq.16)}$$

The anisotropy for our 1 molecule of fluorophore can then be calculated using equation 1.

Now, let us take this scenario one step further by considering a solution mixture of the fluorophore. In a random mixture, for any one particular value of θ we choose to theoretically look at, exciting with plane polarized light will excite all values of ϕ with equal probability. We can therefore calculate the average value of $\sin^2 \phi$ in such a mixture.

$$\sin^2 \phi = \frac{\int_0^{2\pi} \sin^2 \phi \, d\phi}{\int_0^{2\pi} d\phi} = 1/2 \qquad \text{(eq.17)}$$

Consequently for such a scenario;

$$I = \cos^2 \theta$$
$$I = 1/2 \sin^2 \theta \qquad \text{(eq.18)}$$

Now, we want to see what happens when we observe all angles of θ and ϕ. In other words, the average intensities for a random fluorophore mixture would be;

$$I = \cos^2 \theta \qquad \text{(eq.19)}$$
$$I = 1/2 \sin^2 \phi \qquad \text{(eq.20)}$$

Using equation 1 and the identity;$\sin^2 \theta = 1 - \cos^2 \theta$ we arrive at;

$$A = \frac{3 \cos^2 \theta - 1}{2} \qquad \text{(eq.20)}$$

To derive a numerical value for A we must establish the average value of $\cos^2 \theta$. If z-polarized excitational light was able to equally excite all angles of θ, we could then calculate the average value of θ as was done for ϕ and we

would be done with it. In actuality, z-polarized light can excite all angles of θ, however, each angle has a different probability of excitation. The probability of absorption is proportional to $\cos^2 \theta$ (where θ is the angle between the absorption dipole and the z axis). In other words, excitation of a random mixture of fluorophores, selects only for a certain population of fluorophores which are symmetrically distributed about the z axis (Fig.6). This is known as **photoselection.**

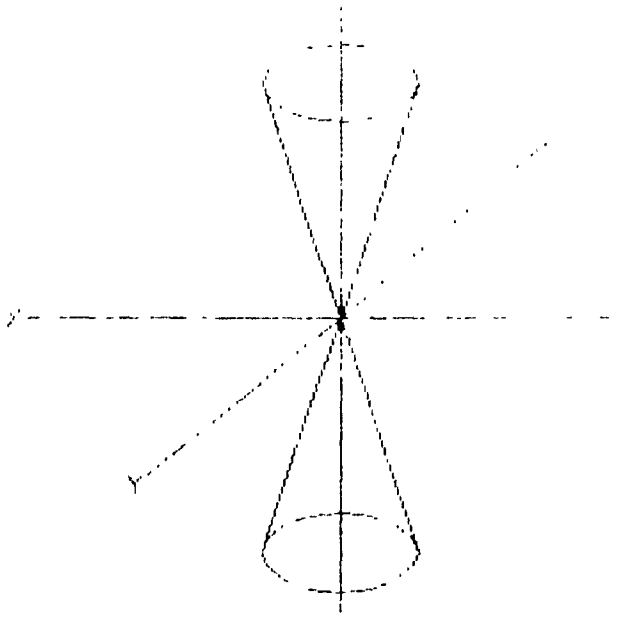

Figure 6: Group of fluorophores excited by z-polarized light.

For a random distribution, the number of molecules at an angle between θ and θ + dθ is proportional to $\sin^2 \theta \, d\theta$ which is proportional to the surface area on a sphere within the angles θ and θ + dθ. The distribution of molecules

excited by vertically polarized light is given by;

$$f(\theta)\, d\theta = \cos^2 \theta \sin \theta \, d\theta \qquad \text{(eq.23)}$$

and consequently;

$$I_{\parallel} = \cos^2 \theta = \frac{\int_0^{2\pi} \cos^2 \theta \, f(\theta) \, d\theta}{\int_0^{2\pi} f(\theta) \, d\theta} = 3/5$$

Substitution into equation 21 gives;

$$A_0 = \frac{3 \cos^2 \theta - 1}{2} = 2/5 \text{ or } 0.4 \qquad \text{(eq.24)}$$

Where A_0 = limiting anisotropy.

The anisotropy of any solution of a fluorophore with collinear dipoles in a vitrified solution will, due to photoselection, be 0.4. We can say that the light has been depolarized from that which would have been observed if z-polarized light solely excited perfectly z-aligned absorption dipoles.The same analysis for polarization yields $P_0 = 0.5$. Since equation 21 is the primal or limiting equation of anisotropy it is given the term A_0, which is the anisotropy in the absence of any depolarizations other than that due to the constant depolarization of

photoselection.

2.2: Anisotropy of fluorophores with noncollinear dipoles in a vitrified solution.

The purpose of this section is to expand equation 21 (and 24) to incorporate nonlinear dipoles.

Equation 21 tells us that for every θ by which the emission dipole is displaced from the z axis the A_0 decreases by; $(3 \cos^2 \theta - 1)/2$. This is an important statement because it means that the nature of the depolarization (either photoselection, nonlinear dipoles, or rotational motion (2.3)) is of no significance. Regardless of the cause of the depolarization the result is a further displacement of θ from the z axis and as such a decrease in A_0 according to equation 21. Mathematically then;

$$A_0 = (2/5) \left(\frac{3 \cos^2 \alpha - 1}{2} \right) \qquad \text{(eq.25)}$$

Where; (2/5) = maximum anisotropy, due to photoselection.

α = intrinsic angle between absorption and emission dipole.

Note:

(1) When $\alpha = 0$ then equation 25 reduces to equation 21

(2) If photoselection did not exist and if $\alpha = 0$ the A_0 would be = 1

(3) The polarization counterpart of equation 25 is;

$$P_0 = (1/2)\left(\frac{6\cos^2\alpha - 2}{\cos^2\alpha + 3}\right)$$

Since the numerical value of $\cos^2\alpha$ alternates between 1 and 0, equations 25 and 26 also tell us that the minimum value of A_0 and P_0 under any circumstance will be -0.20 and -0.33 respectively. We can therefore establish that the range of values under any condition will be:

$$A_0 = -0.20 \text{ to } 0.4$$

and/

$$P_0 = -0.33 \text{ to } 0.5$$

We will next expand equation 25 to encompass fluorophore motion, in a solution of normal viscosity, during the fluorescent lifetime of the fluorophore.

2.3: Anisotropy of a fluorophore bonded to a macromolecule.

Most macromolecules have two important properties in terms of this discussion.

(1) They are capable of rotation on the time scale of fluorescence emission (nanoseconds).

and/

(2) Their rotational motions are not enough to achieve random orientation, of a fluorophore attached to the macromolecule, on the fluorescent time scale.

Consequently, if a fluorophore is rigidly attached to a macromolecule, such that the rotational motion of the macromolecule becomes the rotational motion of the fluorophore, the observed anisotropy of the fluorophore will be some intermediate value between 0.4 and -0.20 or 0.5 and -0.33 for polarization.

To describe the A observed for a fluorophore bonded to a macromolecule one, of course, has to incorporate the macromolecular rotational motion into equation 25. The reader is referred to other texts [20] for the derivations. In any event, the result of the math is to add a $(1 + T_f / T_c)^{-1}$ term to equation 25 to yield:

$$A = 2/5 \left(\frac{3 \cos^2 \alpha - 1}{2} \right) \left(1 + \frac{T_f}{T_c} \right)^{-1} \qquad \text{(eq.28)}$$

Where; T_c = rotational correlation time (nanoseconds) of the macromolecule.

In terms of polarization;

$$P = 1/2 \left(\frac{6 \cos^2 \alpha - 1}{\cos^2 \alpha + 3} \right) \left(1 + \frac{T_f}{T_c} \right)^{-1} \qquad \text{(eq.29)}$$

Since equation 21, as was previously mentioned, is applicable to all depolarizing motions. Equations 28 and 29 can alternatively be stated in their

fully angular terms as:

$$A = 2/5 \left(\frac{3 \cos^2 \alpha - 1}{2} \right) \left(\frac{3 \cos^2 R - 1}{2} \right) \qquad \text{(eq.30)}$$

$$P = 1/2 \left(\frac{6 \cos^2 \alpha - 1}{\cos^2 \alpha + 3} \right) \left(\frac{6 \cos^2 R - 1}{\cos^2 R + 3} \right) \qquad \text{(eq.31)}$$

Where; R = angle through which the macromolecule has rotated during the T_f of the fluorophore. In summary then:

(2/5) = Constant depolarization due to photoselection

$\frac{3 \cos^2 \alpha - 1}{2}$ = Variable depolarization due to angle between absorption and emission dipole

$\frac{3 \cos^2 R - 1}{2} = 1 + \left(\frac{T_f}{T_c} \right)^{-1}$

= Variable depolarization due to macromolecular rotation macromolecular rotation during the T_f of the fluorophore.